(11) Vasey, P. A., Kaye, S. B., Morrison, R., Twelves, C., Wilson, P., Duncan, R., Thomson, A. H., Murray, L. S., Hilditch, T. E., Murray, T., Burtles, S., Fraier, D., Frigerio, E., and Cassidy, J. (1999) Phase I clinical and pharmacokinetic study of PK1 [N-(2-hydroxypropyl)methacrylamide copolymer doxorubicin]: first member of a new class of chemotherapeutic agents – drug-polymer conjugates. *Clin. Cancer Res. 5*, 83–94.
(12) Gordon, A. N., Fleagle, J. T., Guthrie, D., Parkin, D. E., Gore, M. E., and Lacave, A. J. (2001) Recurrent epithelial ovarian carcinoma: a randomized phase III study of pegylated liposomal doxorubicin versus topotecan. *J. Clin. Oncol. 19*, 3312–3322.
(13) Nakanishi, T., Fukushima, S., Okamoto, K., Suzuki, M., Matsumura, Y., Yokoyama, M., Okano, T., Sakurai, Y., and Kataoka, K. (2001) Development of the polymer micelle carrier system for doxorubicin. *J. Controlled Release 74*, 295–302.
(14) Jain, R. K. (1994) Barriers to drug delivery in solid tumors. *Sci. Am. 271*, 58–65.
(15) Takakura, Y., and Hashida, M. (1996) Macromolecular carrier systems for targeted drug delivery: Pharmacokinetic considerations on biodistribution. *Pharm. Res. 13*, 820–831.
(16) Dvorak, H. F., Nagy, J. A., Dvorak, J. T., and Dvorak, A. M. (1998) Identification and characterization of the blood vessels of solid tumors that are leaky to circulating macromolecules. *Am. J. Pathol. 133*, 95–109.
(17) Ishida, T., Kirchmeier, M. J., Moase, E. H., Zalipsky, S., and Allen, T. M. (2001) Targeted delivery and triggered release of liposomal doxorubicin enhances cytotoxicity against human B lymphoma cells. *Biochim. Biophys. Acta Biomembranes 1515*, 144–158.
(18) Tsukioka, Y., Matsumura, Y., Hamaguchi, T., Koike, H., Moriyasu, F., and Kakizoe, T. (2002) Pharmaceutical and biomedical differences between micellar doxorubicin (NK911) and liposomal doxorubicin (Doxil). *Jpn. J. Cancer Res. 93*, 1145–1153.
(19) Unezaki. S., Maruyama, K., Hosoda, J., Nagae, I., Koyanagi, Y., Nakata, M., Ishida, O., Iwatsuru, M., and Tsuchiya, S. (1996) Direct measurement of the extravasation of poly(ethyleneglycol)-coated liposomes into solid tumor tissue by in vivo fluorescence microscopy. *Int. J. Pharm. 144*, 11–17.
(20) Suzuki, H., Nakai, D., Seita, T., and Sugiyama, Y. (1996) Design of a drug delivery system for targeting based on pharmacokinetic consideration. *Adv. Drug Delivery Rev. 19*, 335–357.
(21) Jones, A. T., Gumbleton, M., and Duncan, R. (2003) Understanding endocytic pathways and intracellular trafficking: a prerequisite for effective design of advanced drug delivery systems. *Adv. Drug Delivery Rev. 55*, 1353–1357.
(22) Bae, Y., Fukushima, S., Harada, A., and Kataoka, K. (2003) Design of environment-sensitive supramolecular assemblies for intracellular drug delivery: polymeric micelles that are responsive to intracellular pH change. *Angew. Chem., Int. Ed. 42*, 4640–4643.
(23) D'souza, A. J. M., and Topp, E. M. (2004) Release from polymeric prodrugs: linkages and their degradation. *J. Pharm. Sci. 93*, 1962–1979.
(24) Ulbrich, K., and Subr, V. (2004) Polymeric anticancer drugs with pH-controlled activation. *Adv. Drug Delivery Rev. 56*, 1023–1050.
(25) Willner, D., Trail, P. A., Hofstead, S. J., King, H. D., Lasch, S. J., Braslawsky, G. R., Greenfield, R. S., Kaneko, T., Firestone, R. A. (1993) (6-Maleimidocaproyl)hydrazone of doxorubicin. A new derivative for the preparation of immunoconjugates of doxorubicin. *Bioconjugate Chem. 4*, 521–527.
(26) Kaneko, T., Willner, D., Monkovic, I., Knipe, J. O., Braslawsky, G. R., Greenfield, R. S., and Vyas D. M. (1991) New hydrazone derivatives of adriamycin and their immunoconjugates – a correlation between acid stability and cytotoxicity. *Bioconjugate Chem. 2*, 133–141.
(27) Hamilton, G. (1998) Multicellular spheroids as an in vitro tumor model. *Cancer Lett. 131*, 29–34.
(28) Sutherland, R. M. (1988) Cell and environment interactions in tumor microregions: the multicell spheroid model. *Science 240*, 177–184.
(29) Konerding, M. A., Fait E., and Gaumann, A. (2001) 3D microvascular architecture of pre-cancerous lesions and invasive carcinomas of the colon. *Br. J. Cancer 84*, 1354–1362.
(30) Maeda, H., Wu, J., Sawa, T., Matsumura, Y., and Hori, K. (2000) Tumor vascular permeability and the EPR effect in macromolecular therapeutics: a review. *J. Controlled Release 65*, 271–284.
(31) Matsumura, Y., and Maeda, H. (1986) A new concept of macromolecular therapeutics in cancer chemotherapy: mechanism of tumoritropic accumulation of proteins and the antitumor agent SMANCS. *Cancer Res. 46*, 6387–6392.
(32) Jain, R. K. (1988) Determinants of tumor blood flow: a review. *Cancer Res. 48*, 2641–2658.
(33) Baxter, L. T., Daniel, H. Z., Mackensen, G., and Jain, R. K. (1994) Physiologically based pharmacokinetic model for specific and nonspecific monoclonal antibodies and fragments in normal tissues and human tumor xenografts in nude mice. *Cancer Res. 54*, 1517–1528.
(34) Yamamoto, Y., Nagasaki, Y., Kato, Y., Sugiyama, Y., and Kataoka, K. (2001) Long-circulating poly(ethylene glycol)-poly(D, L-lactide) block copolymer micelles with modulated surface charge. *J. Control. Release 77*, 27–38.
(35) Nishiyama, N., Kato, Y., Sugiyama, Y., and Kataoka, K. (2001) Cisplatin-loaded polymer–metal complex micelle with time-modulated decaying property as a novel drug delivery system. *Pharmaceut. Res. 18*, 1035–1041.
(36) Torchilin, V. P., Lukyanov, A. N., Gao, Z. G., and Papahadjopoulos-Sternberg, B. (2003) Immunomicelles: Targeted pharmaceutical carriers for poorly soluble drugs. *P. Natl. Acad. Sci. USA. 100*, 6039–6044.
(37) Adams, M. L., Lavasanifar, A., and Kwon, G. (2003) Amphiphilic block copolymers for drug delivery. *J. Pharm. Sci. 92*, 1343–1355.
(38) Shiah, J. G., Dvorak, M., Kopeckova, P., Sun, Y., Peterson, C. M., and Kopecek, J. (2001) Biodistribution and antitumour efficacy of long-circulating N-(2-hydroxypropyl)methacrylamide copolymer-doxorubicin conjugates in nude mice. *Eur. J. Cancer 37*, 131–139.
(39) Kopecek, J., Kopeckova, P., Minko, T., Lu, Z. R., and Peterson, C. M. (2001) Water soluble polymers in tumor targeted delivery. *J. Controlled Release 74*, 147–158.
(40) Emanuel, N., Kedar, E., Bolotin, E. M., Smorodinsky, N. I., and Barenholz, Y. (1996) Targeted delivery of doxorubicin via sterically stabilized immunoliposomes: Pharmacokinetics and biodistribution in tumor-bearing mice. *Pharm. Res. 13*, 861–868.
(41) Kataoka, K., Harada, A., and Nagasaki, Y. (2001) Block copolymer micelles for drug delivery: design, characterization and biological significance. *Adv. Drug. Delivery Rev. 47*, 113–131.
(42) Yokoyama, M., Okano, T., Sakurai, Y., Fukushima, S., Okamoto, K., and Kataoka, K. (1999) Selective delivery of adriamycin to a solid tumor using a polymeric micelle carrier system. *J. Drug Target. 7*, 171–186.
(43) Kwon, G., Suwa, S., Yokoyama, M., Okano, T., Sakurai, Y., and Kataoka, K. (1994) Enhanced tumor accumulation and prolonged circulation times of micelle-forming poly(ethylene oxide-aspartate) block copolymer-adriamycin conjugates. *J. Controlled Release 29*, 17–23.

BC0498166

British Journal of Cancer (2005) 92, 1240–1246

www.bjcancer.com

NK105, a paclitaxel-incorporating micellar nanoparticle formulation, can extend *in vivo* antitumour activity and reduce the neurotoxicity of paclitaxel

T Hamaguchi[1], Y Matsumura[*,1,2], M Suzuki[3], K Shimizu[3], R Goda[3], I Nakamura[3], I Nakatomi[4], M Yokoyama[5], K Kataoka[6] and T Kakizoe[7]

[1]Department of Medicine, President of National Cancer Center, 5-1-1 Tsukiji, Chuo-ku, Tokyo 104-0045, Japan; [2]Investigative Treatment Division, National Cancer Center Research Institute East, 6-5-1 Kashiwanoha, Kashiwa, Chiba 277-8577, Japan; [3]Pharmaceuticals Group, Research & Development Division, Nippon Kayaku Co., Ltd, 3-31-12 Shimo, Kita-ku, Tokyo 115-8588, Japan; [4]NanoCarrier Co., Ltd, Tokatsu Techno Plaza, 5-4-6 Kashiwanoha, Kashiwa, Chiba 277-0882, Japan; [5]Kanagawa Academy of Science and Technology, KSP Bldg., East 404, 3-2-1 Sakado, Takatsu-ku, Kawasaki, Kanagawa 213-0012, Japan; [6]Department of Materials Engineering, Graduate School of Engineering, The University of Tokyo, 7-3-1 Hongo, Bunkyo-ku, Tokyo 113-8656, Japan; [7]President of National Cancer Center, 5-1-1 Tsukiji, Chuo-ku, Tokyo 104-0045, Japan

Paclitaxel (PTX) is one of the most effective anticancer agents. In clinical practice, however, high incidences of adverse reactions of the drug, for example, neurotoxicity, myelosuppression, and allergic reactions, have been reported. NK105, a micellar nanoparticle formulation, was developed to overcome these problems and to enhance the antitumour activity of PTX. Via the self-association process, PTX was incorporated into the inner core of the micelle system by physical entrapment through hydrophobic interactions between the drug and the well-designed block copolymers for PTX. NK105 was compared with free PTX with respect to their *in vitro* cytotoxicity, *in vivo* antitumour activity, pharmacokinetics, pharmacodynamics, and neurotoxicity. Consequently, the plasma area under the curve (AUC) values were approximately 90-fold higher for NK105 than for free PTX because the leakage of PTX from normal blood vessels was minimal and its capture by the reticuloendothelial system minimised. Thus, the tumour AUC value was 25-fold higher for NK105 than for free PTX. NK105 showed significantly potent antitumour activity on a human colorectal cancer cell line HT-29 xenograft as compared with PTX ($P<0.001$) because the enhanced accumulation of the drug in the tumour has occurred, probably followed by its effective and sustained release from micellar nanoparticles. Neurotoxicity was significantly weaker with NK105 than with free PTX. The neurotoxicity of PTX was attenuated by NK105, which was demonstrated by both histopathological ($P<0.001$) and physiological ($P<0.05$) methods for the first time. The present study suggests that NK105 warrants a clinical trial for patients with metastatic solid tumours.
British Journal of Cancer (2005) **92,** 1240–1246. doi:10.1038/sj.bjc.6602479 www.bjcancer.com
Published online 22 March 2005

Keywords: NK105; paclitaxel; polymer micelles; DDS; EPR effect

Paclitaxel (PTX) is one of the most useful anticancer agents known for various cancers including ovarian, breast, and lung cancers (Carney, 1996; Khayat *et al*, 2000). However, PTX has serious adverse effects, for example, neutropenia and peripheral sensory neuropathy. In addition, anaphylaxis and other severe hypersensitive reactions have been reported to develop in 2–4% of patients receiving the drug even after premedication with antiallergic agents; these adverse reactions have been attributed to the mixture of Cremophor EL and ethanol, which was used to solubilise PTX (Weiss *et al*, 1990; Rowinsky and Donehower, 1995). Of the adverse reactions, neutropenia can be prevented or managed effectively by administering a granulocyte colony-stimulating factor. On the other hand, there are no effective therapies to prevent or reduce nerve damage, which is associated with peripheral neuropathy caused by PTX; therefore, neurotoxicity constitutes a significant dose-limiting toxicity of the drug (Rowinsky *et al*, 1993; Wasserheit *et al*, 1996).

The above problems of PTX have been attributed to its low therapeutic indices and limited efficacy due to the nonselective nature of its therapeutic targets and its inability to accumulate selectively in cancer tissue. Therefore, there is an urgent need to develop modalities by which cytotoxic drugs can selectively target tumour tissue and effectively act on cancer cells in the scene. The roles of drug delivery systems (DDSs) have drawn attention in this context. Drug delivery systems are based on two main principles: active and passive targetings. The former refers to the development of monoclonal antibodies directed against tumour-related molecules that allow targeting of the tumour because of specific binding between the antibody and its antigen. However, the application of

*Correspondence: Dr Y Matsumura, Investigative Treatment Division, National Cancer Center Research Institute East, 6-5-1 Kashiwanoha, Kashiwa, Chiba 277-8577, Japan; E-mail: yhmatsum@east.ncc.go.jp
Received 27 October 2004; revised 26 January 2005; accepted 31 January 2005; published online 22 March 2005

DDSs using monoclonal antibodies is restricted to tumours expressing high levels of related antigens.

Passive targeting is based on the so-called enhanced permeability and retention (EPR) effect (Matsumura and Maeda, 1986; Maeda *et al*, 2000). The EPR effect consists in the pathophysiological characteristics of solid tumour tissue: hypervascularity, incomplete vascular architecture, secretion of vascular permeability factors stimulating extravasation within cancer tissue, and absence of effective lymphatic drainage from tumours that impedes the efficient clearance of macromolecules accumulated in solid tumour tissues.

Several techniques to maximally use the EPR effect have been developed, that is, modification of drug structures and development of drug carriers. The first micelle-forming polymeric drug developed was polyethylene glycol (PEG)-polyaspartate block copolymer conjugated with doxorubicin (DXR) (Yokoyama *et al*, 1990; Yokoyama *et al*, 1991; Kataoka *et al*, 1993). PEG constituted the outer shell of the micelle, which conferred a stealth property on the drug that allowed the micellar drug preparations to be less avidly taken up by the reticuloendothelial system (RES) and to be retained in the circulation for a longer time. Prolonged circulation time and the ability of polymeric micelles to extravasate through the leaky tumour vasculature were expected to result in the accumulation of DXR in tumour tissue due to the EPR effect (Kwon *et al*, 1994; Yokoyama *et al*, 1999). A clinical trail of micellar DXR, NK911, is now underway (Nakanishi *et al*, 2001; Hamaguchi *et al*, 2003). Recently, we succeeded in constructing NK105, a polymeric micelle carrier system for PTX, which conferred on PTX a passive targeting ability based on the EPR effect. In the present paper, we describe the details and characteristics of NK105. We also discuss differences between NK105 and other DDS formulations containing PTX.

MATERIALS AND METHODS

Materials

PTX was purchased from Mercian Corp. (Tokyo, Japan). All other chemicals were of reagent grade. Following cell lines, MKN-45, MKN-28, HT-29, DLD-1, HCT116, TE-1, TE-8, PC-14, PC-14/TXT, H460, MCAS, OVCAR-3, AsPC-1, PAN-9, PAN-3, and MCF-7 cells were purchased from American Type Culture Collection. Colon 26 cells were dispensed from the Japan Foundation for Cancer Research (Tokyo, Japan). Female BALB/c *nu/nu* mice were purchased from SLC (Shizuoka, Japan). Female CDF1 mice and IGS rats were purchased from Charles River Japan Inc. (Kanagawa, Japan).

All animal procedures were performed in compliance with the guidelines for the care and use of experimental animals, which had been drawn up by the Committee for Animal Experimentation of the National Cancer Center; these guidelines meet the ethical standards required by law and also comply with the guidelines for the use of experimental animals in Japan.

NK105, a PTX-incorporating micellar nanoparticle formulation

NK105 is a PTX-incorporating 'core-shell-type' polymeric micellar nanoparticle formulation. Polymeric micellar particles were formed by facilitating the self-association of amphiphilic block copolymers in an aqueous medium. Novel amphiphilic block copolymers, namely NK105 polymers, were designed for PTX entrapment. NK105 polymers were constructed using PEG as the hydrophilic segment and modified polyaspartate as the hydrophobic segment. Carboxylic groups of polyaspartate block were modified with 4-phenyl-1-butanol by esterification reaction, consequently the half of the groups were converted to 4-phenyl-1-butanolate. Via the self-association process, PTX was incorporated into the inner core of the micelle system by physical entrapment through hydrophobic interactions between the drug and specifically well-designed block copolymers for PTX.

Pharmacokinetics and pharmacodynamics of PTX and NK105

Colon 26 tumour-bearing CDF1 mice aged 8 weeks were given intravenously (i.v.) via the tail vein PTX 50 and 100 mg kg^{-1} or NK105 at corresponding PTX-equivalent doses. Mice were killed at 5 and 30 min, as well as 2, 6, 24, and 72 h after injection. Blood was collected, and tumours were removed; plasma and tumours obtained were then stored at −20°C until the analysis. Each time point for collection represented three samples from three different mice. PTX was extracted from plasma obtained by deproteinisation using acetonitrile, followed by liquid–liquid extraction with *t*-butylmethylether. Tumours obtained were homogenised in 0.5% acetic acid, and the resultant homogenate was deproteinised and extracted according to the same method as that used for plasma. The blood and tumour extracts were analysed for PTX by liquid chromatography/tandem mass spectrometry. Reversed-phase column-switching chromatography was conducted using an ODS column and detection was enabled by electrospray ionisation of positive mode. The mean plasma and tumour concentrations of PTX at each sampling point were calculated for both PTX and NK105. Pharmacokinetic modelling was completed using a WinNonlin Standard software version 3.1 (Pharsight Corp., California, USA).

In vitro cytotoxicity

Various human cancer cell lines were evaluated in the present study. The cell lines were maintained in monolayer cultures in Dulbecco's modified Eagle's medium containing 10% (v v^{-1}) foetal calf serum and 600 mg l^{-1} glutamine. WST-8 Cell Counting Kit-8 (Dojindo, Kumamoto, Japan) was used for the cell proliferation assay. In all, 2000 cells of each cell line in 90 μl of culture medium were plated in 96-well plates and were then incubated for 24 h at 37°C. Serial dilutions of PTX or NK105 in a volume of 10 μl were added, and the cells were incubated for 48 or 72 h. All data were expressed as mean ± s.e. of triplicate cultures. The data were then plotted as a percentage of the data from the control cultures, which were treated identically to the experimental cultures, except that no drug was added.

Evaluation of the antitumour activity of PTX and NK105

The antitumour activity of PTX and NK105 was evaluated using nude mice implanted with a human colonic cancer cell line, HT-29. One million tumour cells of HT-29 were inoculated at a subcutaneous (s.c.) site on the back skin of BALB/c female nude mice aged 6 weeks. When tumour size reached approximately 5–8 mm in diameter, mice were randomly allocated to the PTX administration group, NK105 administration group, and control administration group, each of which was made up of five animals. Each treatment was carried out as follows: free PTX group was administered at a dose of 25, 50, or 100 mg kg^{-1}; NK105 group was with same PTX-equivalent doses; and in control group, animals were given saline. Mice were administered a single i.v. injection of PTX or NK105 weekly for 3 weeks. The antitumour activity of PTX and NK105 was evaluated by measuring tumour size ($a \times b$, where a is the major diameter and b is the minor diameter) at various time points after injection. Changes in body weight were also monitored for mice, which were used in the present study.

Evaluation of neurotoxicity

The severity of neurotoxicity was assessed both electrophysiologically and histologically. Under intraperitoneal ketamine anaesthesia (40 mg kg^{-1}), rats were given a single i.v. injection of PTX (7.5 mg kg^{-1}), NK105 (a PTX-equivalent dose of 7.5 mg kg^{-1}), or 5% glucose weekly for 6 weeks. All the solutions were administered through the jugular vein exposed via a small incision in the neck. Electrophysiological measurements were conducted 1 day before the first dosing and on day 6 after the final dosing. For electrophysiological recording, rats were anaesthetised by the intraperitoneal injection of pentobarbital 40 mg kg^{-1}. Electrical stimuli were given peripherally, and caudal sensory nerve action potentials (caudal SNAPs) were recorded centrally from the tail. The amplitude of each waveform was calculated by measuring the caudal SNAP from the top peak to the bottom peak. Variations in the amplitude after the 6th weekly administration of the solutions were determined.

For light microscopy, rats were killed after electrophysiological recordings. Subsequently, a segment of the sciatic nerve was carefully removed, and embedded in paraffin. Sections (2 μm thick) were stained with haematoxylin and eosin (H & E) before examination under light microscopy to evaluate the degenerative changes of myelinated nerve fibres.

Statistical analysis

The data of therapeutic efficacy was expressed as mean $\pm$ s.e.m. The statistical significance of differences in therapeutic efficacy between two administration groups was calculated by means of repeated measures (analysis of variance). The statistical significance of the differences in neurotoxic activity between two administration groups was calculated using the Student's *t*-test on the closed testing procedure. The histopathological impairment was scored in five grades. The statistical significance of the differences in histopathological impairment between two administration groups was calculated using the Wilcoxon's rank-sum test on the closed testing procedure. All data were calculated with software StatView, version 5 (ABACUS Concepts, Berkeley, CA, USA). A value of $P<0.05$ was considered statistically significant.

RESULTS

Preparation and characterisation of NK105

To construct NK105 micellar nanoparticles (Figure 1A), block copolymers consisting of PEG and polyaspartate, the so-called PEG polyaspartate described previously (9, 11, 13, 14), were used. PTX was incorporated into polymeric micelles formed by physical entrapment utilising hydrophobic interactions between PTX and the block copolymer polyaspartate chain. After screening of many candidate substances, 4-phenyl-1-butanol was employed for the chemical modification of the polyaspartate block to increase its hydrophobicity. Treating with a condensing agent, 1,3-diisopropylcarbodiimide, the half of carboxyl groups on the polyaspartate, was esterified with 4-phenyl-1-butanol. Molecular weight of the polymers was determined to be approximately 20 000 (PEG block: 12 000; modified polyaspartate block: 8000). NK105 was prepared by facilitating the self-association of NK105 polymers and PTX. NK105 was obtained as a freeze-dried formulation and contained ca. 23% (w w^{-1}) of PTX, as determined by reversed-phase liquid chromatography using an ODS column with mobile phase consisting of acetonitrile and water (9 : 11, v v^{-1}) and detection of ultraviolet absorbance at 227 nm. Finally, NK105, a PTX-incorporating polymeric micellar nanoparticle formulation with a single and narrow size distribution, was obtained. The weight-average diameter of the nanoparticles was approximately 85 nm ranging from 20 to 430 nm (Figure 1B).

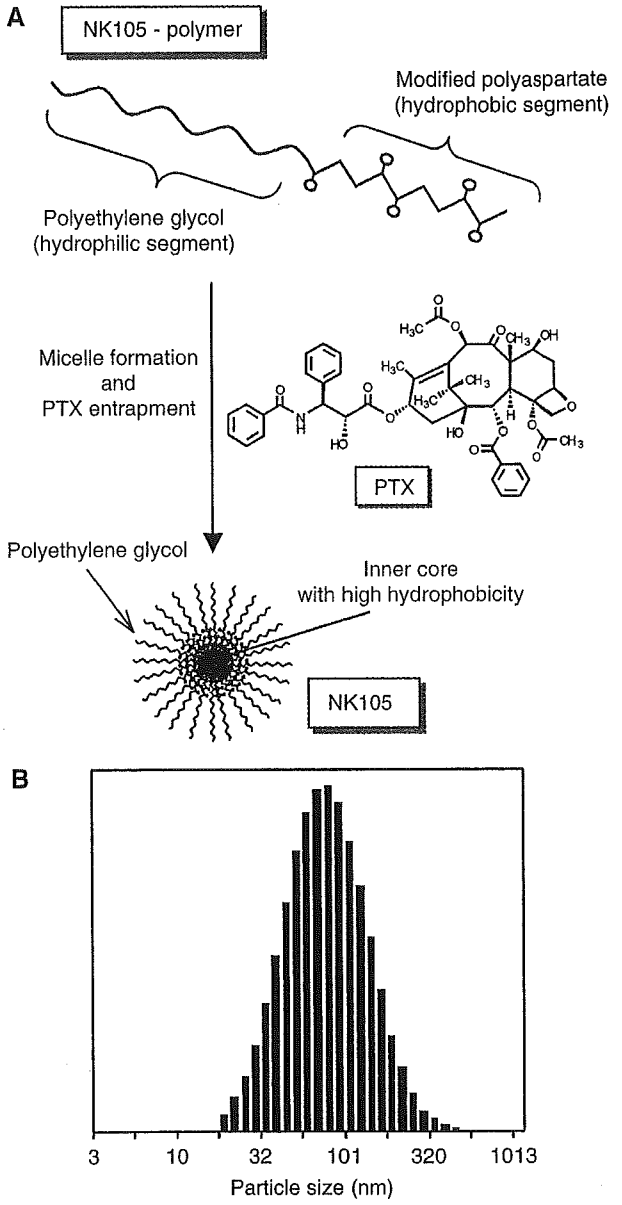

Figure 1 Preparation and characterisation of NK105. (**A**) The micellar structure of NK105 PTX was incorporated into the inner core of the micelle. (**B**) The size distribution of NK105 measured by the dynamic light scattering method. The mean diameter of an NK105 micelle was 85 nm.

Pharmacokinetics and pharmacodynamics of NK105

Colon 26-bearing CDF1 mice were given a single i.v. injection of PTX 50 or 100 mg kg^{-1}, or of NK105 at an equivalent dose of PTX. Subsequently, the time-course changes in the plasma and tumour levels of PTX were determined in the PTX and NK105 administration groups (Figure 2); furthermore, the pharmacokinetic parameters of each group were also determined (Table 1). NK105 exhibited slower clearance from the plasma than PTX, while NK105 was present in the plasma for up to 72 h after injection; PTX was not detected after 24 h or later of injection. The plasma concentration at 5 min ($C_{5\,min}$) and the area under the curve (AUC) of NK105 were 11–20-fold and 50–86-fold higher for NK105 than for PTX, respectively. Furthermore, the half-life at the terminal phase ($t_{1/2}z$) was 4–6 times longer for NK105 than for

PTX. The maximum concentration (C_{max}) and AUC of NK105 in Colon 26 tumours were approximately 3 and 25 times higher for NK105 than for PTX, respectively. NK105 continued to accumulate in the tumours until 72 h after injection. The tumour PTX concentration was higher than 10 $\mu g\,g^{-1}$ even at 72 h after the i.v. injection of NK105 50 and 100 $mg\,kg^{-1}$. On the contrary, the tumour PTX concentrations at 72 h after the i.v. administration of free PTX 50 and 100 $mg\,kg^{-1}$ were below detection limits and less than 0.1 $\mu g\,g^{-1}$, respectively.

In vitro cytotoxicity

NK105 was tested on 12 human tumour cell lines derived from lung, gastric, oesophagus, colon, breast, and ovarian tumours. Similar dose–response curves were noted for PTX and NK105 (data not shown). Furthermore, the IC_{50} values of NK105 were similar to those of PTX at 48 and 72 h, indicating that both NK105 and PTX showed equivalent cytotoxic activity *in vitro* (Table 2).

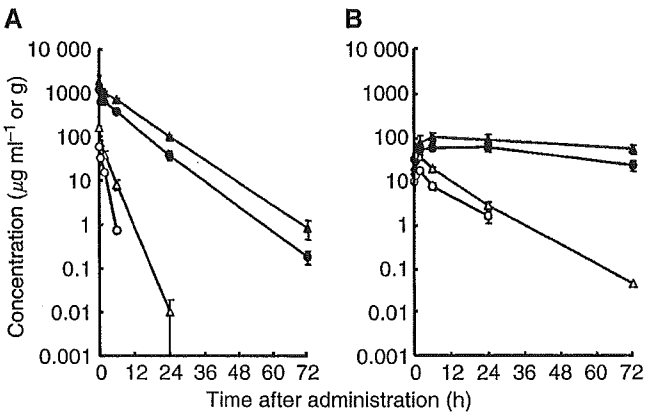

Figure 2 Plasma and tumour concentrations of PTX after single i.v. administration of NK105 or PTX to Colon 26-bearing CDF1 mice. Plasma (**A**) and tumour (**B**) concentrations of PTX after NK105 administration at a PTX-equivalent dose of 50 $mg\,kg^{-1}$ (●), NK105 at a PTX-equivalent dose of 100 $mg\,kg^{-1}$ (▲), PTX 50 $mg\,kg^{-1}$ (○) and PTX 100 $mg\,kg^{-1}$ (△).

In vivo antitumour activity

BALB/c mice bearing s.c. HT-29 colon cancer tumours showed decreased tumour growth rates after the administration of PTX and NK105. However, NK105 exhibited superior antitumour activity as compared with PTX ($P<0.001$). The antitumour activity of NK105 administered at a PTX-equivalent dose of 25 $mg\,kg^{-1}$ was comparable to that obtained after the administration of free PTX 100 $mg\,kg^{-1}$. Tumour suppression by NK105 increased in a dose-dependent manner. Tumours disappeared after the first dosing to mice treated with NK105 at a PTX-equivalent dose of 100 $mg\,kg^{-1}$, and all mice remained tumour-free thereafter (Figure 3A). In addition, less weight loss was induced in mice, which were given NK105 100 $mg\,kg^{-1}$ than in those that were given the same dose of free PTX (Figure 3B).

Table 2 IC_{50} values (μM) of PTX and NK105 in various cell lines

		48 h		72 h	
Cancer	**Cell line**	**NK105**	**PTX**	**NK105**	**PTX**
Oesophageal cancer	TE-1	>1.0	>1.0	0.01	0.02
	TE-8	0.02	0.02	0.01	0.01
Lung cancer	PC-14	0.01	0.01	0.01	0.01
	PC-14/TXT	0.15	0.09	0.08	0.06
	H460	ND	ND	0.03	0.01
Breast cancer	MCF-7	>1.0	>1.0	0.01	0.01
Stomach cancer	MKN-28	0.03	0.03	0.01	0.21
	MKN-45	0.02	0.07	0.01	0.02
Colon cancer	DLD-1	0.95	0.26	0.29	0.20
	HT-29	0.01	0.01	0.01	0.01
	HCT116	ND	ND	0.03	0.01
Ovarian cancer	MCAS	0.01	0.01	0.01	0.01
	OVCAR-3	>1.0	>1.0	>1.0	>1.0
Pancreatic cancer	AsPC-1	ND	ND	0.02	0.02
	PAN-9	ND	ND	0.03	0.02
	PAN-3	ND	ND	0.010	0.004

PTX = paclitaxel; ND = not done.

Table 1 Pharmacokinetic parameters for the plasma and tumour concentrations of paclitaxel after single i.v. administration of NK105 and PTX to Colon 26-bearing CDF1 mice

Treatment	**Dose ($mg\,kg^{-1}$)**	**$C_{5\,min}$ ($\mu g\,ml^{-1}$)**	**$t_{1/2}z$ (h)**	**AUC_{0-t} ($\mu g\,h\,ml^{-1}$)**	**$AUC_{0-inf.}$ ($\mu g\,h\,ml^{-1}$)**	**CL_{tot} ($ml\,h\,kg^{-1}$)**	**V_{ss} ($ml\,kg^{-1}$)**
Plasma							
PTX	50	59.32	0.98	90.2[a]	91.3	547.6	684.6
PTX	100	157.67	1.84	309.0[b]	309.0	323.6	812.2
NK105	50	1157.03	5.99	7860.9[c]	7862.3	6.4	46.4
NK105	100	1812.37	6.82	15565.7[c]	15573.6	6.4	54.8
		C_{max} ($\mu g\,ml^{-1}$)	**T_{max} (h)**	**$t_{1/2}z$ (h)**	**AUC_{0-t} ($\mu g\,h\,ml^{-1}$)**	**$AUC_{0-inf.}$ ($\mu g\,h\,ml^{-1}$)**	
Tumour							
PTX	50	12.50	2.0	7.02	120.8[b]	133.0	
PTX	100	28.57	0.5	8.06	330.4[c]	331.0	
NK105	50	42.45	24.0	35.07	2360.1[c]	3192.0	
NK105	100	71.09	6.0	73.66	3884.9[c]	7964.5	

i.v. = intravenous; $C_{5\,min}$ = plasma concentration at 5 min; $t_{1/2}z$ = half-life at the terminal phase; AUC = area under the curve; CL_{tot} = total body clearance; V_{ss} = volume of distribution at steady state; T_{max} = time of maximum concentration; PTX = paclitaxel. Parameters were calculated from the mean value of three or two mice by noncompartmental analysis. [a]$AUC_{0\text{-}6h}$. [b]AUC_{0-24h}. [c]AUC_{0-72h}.

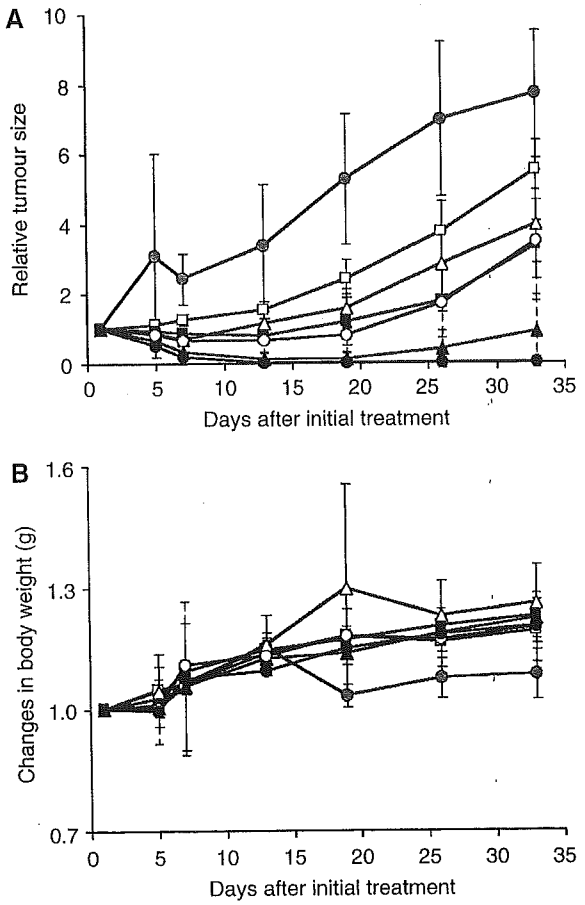

Figure 3 Relative changes in HT-29 tumour growth rates in nude mice. (**A**) Effects of PTX (open symbols) and NK105 (closed symbols). PTX and NK105 were injected i.v. once weekly for 3 weeks at PTX-equivalent doses of 25 mg kg^{-1} (□, ■), 50 mg kg^{-1} (△, ▲), and 100 mg kg^{-1} (○, ●), respectively. Saline was injected to control animals (●). (**B**) Changes in relative body weight. Data were derived from the same mice as those used for the present study.

Neurotoxicity of PTX and NK105

Treatment with PTX has resulted in cumulative sensory-dominant peripheral neurotoxicity in humans, characterised clinically by numbness and/or paraesthesia of the extremities. Pathologically, axonal swelling, vesicular degeneration, and demyelination were observed. We, therefore, examined the effects of free PTX and NK105 using both electrophysiological and morphological methods.

Prior to drug administration, there were no significant differences in the amplitude of caudal sensory nerve action potential (caudal SNAP) between two drug administration groups. On day 6 after the last dosing (at week 6), the amplitude of the caudal SNAP in the control group increased in association with rat maturation. The amplitude was significantly smaller in the PTX group than in the control group ($P<0.01$), while the amplitude was significantly larger in the NK105 group than in the PTX group ($P<0.05$) and was comparable between the NK105 group and the control group (Figure 4A). Histopathological examination of longitudinal paraffin-embedded sections of the sciatic nerve 5 days after the sixth weekly injection revealed degenerative changes. The NK105 administration group showed only a few degenerative myelinated fibres in contrast to the PTX administration group, which indicated markedly more numerous degenerative myelinated fibres ($P<0.001$) (Figure 4B and C) and Table 3.

DISCUSSION

A pharmacokinetic study revealed that the plasma AUC of NK105 was approximately 90-fold higher than that of free PTX in the present rodent models. Prolonged circulation of NK105 in the blood due to the EPR effect was associated with a significant increase in the tumour AUC. In fact, the tumour AUC of NK105 was approximately 25-fold higher than that of free PTX (Figure 2B). In mice, accordingly, NK105 exhibited stronger antitumour activity than free PTX (Figure 3A). However, it is still debatable whether or not the enhanced accumulation of an anticancer drug into a tumour is sufficient in leading the drug to exert its antitumour activity *in vivo*.

Jain *et al* have reported that the convective passage of large drug molecules into the core of solid tumours could be impeded by abnormally high interstitial pressures in solid tumours. However, they also admitted that low-molecular-weight anticancer agents might be harmful to normal organs because they can leak out of normal blood vessels freely; they finally concluded that one useful strategy for evading the barriers to drug dispersion would be to inject patients with drug carriers, such as liposomes, filled with low-molecular-weight drugs (Jain, 1994). In this case, liposomes should have sufficient time to exit from the site of tumour blood vessel leakage and to accumulate at reasonably high dose levels in the surrounding interstitium. Subsequently, low-molecular-weight drugs packed within liposomes should be released gradually so that they can be dispersed throughout the tumour. However, Unezaki *et al* have used fluorescence-labelled PEG-liposomes and described that the area of highest fluorescence was located outside tumour vessels, almost all around the vessel wall, even 2 days after drug injection (Unezaki *et al*, 1996). Therefore, the study suggested that although PEG-liposomes can be delivered effectively to a solid tumour via the EPR effect, the formulation would not be distributed sufficiently to cancer cells distant from tumour vessels because liposomes are too large to scamper about in the tumour interstitium. Liposomes have been suggested to be too stable to allow the drug therein to be released easily. Therefore, PEG-liposomes have been speculated to be not so effective against cancers in which the tumour vessel network is irregular and loose because of an abundant collagen-rich matrix. Such cancers include scirrhous cancer of the stomach and pancreatic cancer. In fact, Doxil®, a PEG-liposomal DXR, is known to be effective clinically against ovarian cancer and breast cancer, both of which are characterised by a high density of tumour microvessels; however, the drug is not effective against stomach cancer and pancreatic cancer (Muggia, 2001).

There are several possible reasons why NK105 exhibited higher antitumour activity in the present study as compared with free PTX: (1) since NK105 is very stable in the circulation and exhibits a markedly higher plasma AUC than free PTX, it accumulates better in tumour tissue than does free PTX due to the EPR effect; (2) NK105 is relatively small in size (85 nm) as compared with Doxil (100 nm), thus explaining its more uniform distribution in tumour tissue and its greater accumulation in cancer cells throughout cancer tissue. Savic *et al* (2003) have recently reported that polymeric micelles could internalise into cells to localise in several cytoplasmic organelles; and (3) a polymeric micelle carrier system for a drug has the potential to allow the effective sustained release of the drug inside a tumour following the accumulation of micelles into tumour tissue. Regarding NK105 in particular, this sustained release begins at a PTX-equivalent dose of $<1\,\mu g\,ml^{-1}$ (data not shown). Consequently, released PTX becomes distributed throughout tumour tissue and internalises into cancer cells to kill them.

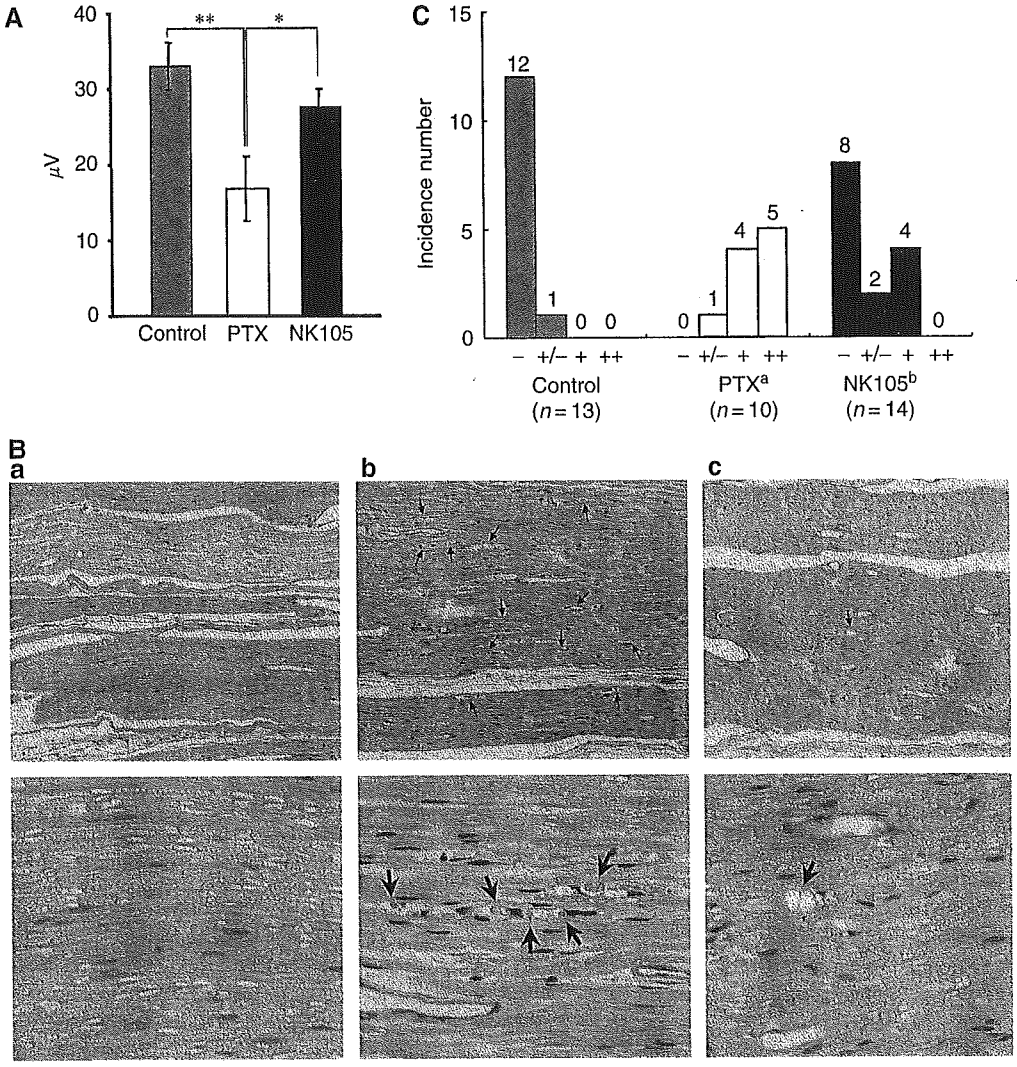

Figure 4 Incorporation of PTX into polymeric micelles diminishes neurotoxicity. (**A**) Effects of PTX or NK105 on the amplitude of rat caudal sensory nerve action potentials as examined 5 days after weekly injections for 6 weeks. Rats ($n=14$) were injected with NK105 (■) or PTX (□) at a PTX-equivalent dose of 7.5 mg kg^{-1}. Glucose (5%) was also injected in the same manner to animals in the control group (■). *$P<0.05$, **$P<0.01$. (**B**) Histopathological changes in the sciatic nerve of rats. Degenerating myelinated nerve fibres (arrow) were examined in the longitudinal section of the sciatic nerve (H & E) 5 days after weekly injections for 6 weeks with 5% glucose (a), PTX (b), and NK105 (c) at a PTX-equivalent dose of 7.5 mg kg^{-1}. Magnification, × 100 (upper) and × 400 (lower). (**C**) Incidences of degenerating myelinated nerve fibres in rats treated with PTX or NK105. NK105 or PTX was administered i.v. at a weekly dose of 7.5 mg kg^{-1} for 6 consecutive weeks to female rats. The degenerating myelinated fibre score was defined as follows: –, no degenerative changes; +/–, very slight degree of the degenerative changes (scattered, single fibres affected); +, slight degree of degenerative changes (scattered small groups of degenerative myelinated fibres); + +, moderate degree of degenerative changes (disseminated degenerative myelinated fibres); + + +, marked degree of degenerative changes (confluent groups of affected fibres). [a]$P<0.001$ *vs* vehicle-treated animals. [b]$P<0.001$ *vs* PTX-treated animals.

To date, PTX preparations that are categorised to DDSs have been developed. Among them, clinical trials are currently ongoing for the following drugs: CT-2103, polyglutamate-conjugated PTX (Singer *et al*, 2003); ABI-007, PTX coated with albumin (Ibrahim *et al*, 2002); and Genexol-PM, PTX micelle in which PTX is simply solubilised (Kim *et al*, 2004). The advantage commonly shared with these dosage forms is that they are injectable i.v. without the mixture of Cremophor EL and ethanol, which potentially provoke serious allergic reactions. The block copolymer used for forming NK105 micellar nanoparticles is nonimmunogenic and is injectable i.v. without Cremorphor EL and ethanol. Therefore, this dosage form is expected to possess a clinical advantage, which is similar to that of the above PTX dosage forms. Now, what is the difference between NK105 and other PTX dosage forms? ABI-007 and Genexol-PM were found to have the AUC and tumour AUC, which are nearly comparable or rather slightly lower than those of free PTX. Furthermore, the plasma AUC and tumour AUC are 11.5- and 11.8-fold higher, respectively, for CT-2103 than for free PTX, but they are markedly low as compared with those of NK105. Respective studies have employed proper tumours and proper rodent models. However, NK105 was forecasted to have markedly high plasma and tumour AUC as compared with those of other PTX dosage forms.

Regarding the toxicity profiles, the repeated administration of NK105 to rats at 7-day intervals produced less toxic effects on peripheral nerves than free PTX. This reduced the neurotoxicity of

Table 3 Incidence of degenerating myelinated fibres in rats treated with PTX or NK105

		Degenerating myelinated nerve fibre score[b]				
Treatment	***n*[a]**	**–**	**+/–**	**+**	**++**	**+++**
Control (vehicle)	13	12	1			
PTX[c]	10		1	4	5	
NK105[d]	14	8	2	4		

PTX = paclitaxel. Vehicle, NK105 or PTX was administered i.v. at a weekly dose of 7.5 mg kg^{-1} for 6 consecutive weeks to female rats. [a]Total number of animals accounted for that experimental condition. [b]Degenerating myelinated fibre score was defined as follows: –, no degenerative changes; +/–, very slight degree of the degenerative changes (scattered, single fibres affected); +, slight degree of degenerative changes (scattered small groups of degenerative myelinated fibers); ++, moderate degree of degenerative changes (disseminated degenerative myelinated fibers); +++, marked degree of degenerative changes (confluent groups of affected fibres). [c]$P<0.001$ *vs* vehicle-treated animals. [d]$P<0.001$ *vs* PTX-treated animals.

NK105, which was demonstrated for the first time by bot histopathological and physiological methods and was probab attributable to the less distribution of PTX into normal neur tissue following NK105 administration, since the volume distribution at steady state (V_{ss}) of NK105 was 100-fold low than that of free PTX. Regarding bone marrow toxicity, there w no difference between PTX and NK105 when 37.5 mg kg^{-1} of PT equivalent dose was administered to rats weekly for 4 consecuti weeks (data not shown). These data indicate that NK105 warrants clinical evaluation.

ACKNOWLEDGEMENTS

We thank Dr H Uchino, Miss M Araake, and Mrs H Koike for the technical assistance. We are also grateful to Mrs K Shiina and Mis H Orita for their secretarial assistance. This work was supporte by a Grant-in-Aid from the Ministry of Health, Labor and Welfa of Japan (Y Matsumura).

Translational Therapeutics

REFERENCES

Carney DN (1996) Chemotherapy in the management of patients with inoperable non-small cell lung cancer. *Semin Oncol* **23:** 71–75

Hamaguchi T, Matsumura Y, Shirao Y, Shimada Y, Yamada Y, Muro Y, Okusaka T, Ueno H, Ikeda M, Watanabe N (2003) Phase I study of novel drug delivery system, NK911, a polymer micelle encapsulated doxorubicin. *Proc Am Soc Clin Oncol* **22:** 571

Ibrahim NK, Desai N, Legha S, Soon-Shiong P, Theriault RL, Rivera E, Esmaeli B, Ring SE, Bedikian A, Hortobagyi GN, Ellerhorst JA (2002) Phase I and pharmacokinetic study of ABI-007, a Cremophor-free, protein-stabilized, nanoparticle formulation of paclitaxel. *Clin Cancer Res* **8:** 1038–1044

Jain RK (1994) Barriers to drug delivery in solid tumours. *Sci Am* **271:** 58–65

Kataoka K, Kwon GS, Yokoyama M, Okano T, Sakurai Y (1993) Block copolymer micelles as vehicles for drug delivery. *J Control Rel* **24:** 119–132

Khayat D, Antoine EC, Coeffic D (2000) Taxol in the management of cancers of the breast and the ovary. *Cancer Invest* **18:** 242–260

Kim TY, Kim DW, Chung JY, Shin SG, Kim SC, Heo DS, Kim NK, Bang YJ (2004) Phase I and pharmacokinetic study of Genexol-PM, a cremophor-free, polymeric micelle-formulated paclitaxel, in patients with advanced malignancies. *Clin Cancer Res* **10:** 3708–3716

Kwon GS, Suwa S, Yokoyama M, Okano T, Sakurai Y (1994) Enhanced tumour accumulation and prolonged circulation times of micelle-forming poly(ethylene oxide-aspartic) block copolymer–adriamycin conjugate. *J Control Rel* **29:** 17–23

Maeda H, Wu J, Sawa T, Matsumura Y, Hori K (2000) Tumour vascular permeability and the EPR effect in macromolecular therapeutics: a review. *J Control Rel* **65:** 271–284

Matsumura Y, Maeda H (1986) A new concept for macromolecular therapeutics in cancer chemotherapy: mechanism of tumouritropic accumulation of proteins and the antitumour agent smancs. *Cancer Res* **46:** 6387–6392

Muggia FM (2001) Liposomal encapsulated anthracyclines: new therapeutic horizons. *Curr Oncol Rep* **3:** 156–162

Nakanishi T, Fukushima S, Okamoto K, Suzuki M, Matsumura Y, Yokoyama M, Okano T, Sakurai Y, Kataoka K (2001) Development of the polymer micelle carrier system for doxorubicin. *J Control Rel* **74:** 295–302

Rowinsky EK, Chaudhry V, Forastiere AA, Sartorius SE, Ettinger D Grochow LB, Lubejko BG, Cornblath DR, Donehower RC (1993) Phase and pharmacologic study of paclitaxel and cisplatin with granulocyt colony-stimulating factor: neuromuscular toxicity is dose-limiting. *J Cli Oncol* **11:** 2010–2020

Rowinsky EK, Donehower RC (1995) Paclitaxel (taxol). *N Engl J Med* **33** 1004–1014

Savic R, Luo L, Eisenberg A, Maysinger D (2003) Micellar nanocontaine distribute to defined cytoplasmic organelles. *Science* **300:** 615–618

Singer JW, Baker B, De Vries P, Kumar A, Shaffer S, Vawter E, Bolton M Garzone P (2003) Poly-(L)-glutamic acid-paclitaxel (CT-2103) [XYC TAX], a biodegradable polymeric drug conjugate: characterizatio preclinical pharmacology, and preliminary clinical data. *Adv Exp Me Biol* **519:** 81–99

Unezaki S, Maruyama K, Hosoda J, Nagai I, Koyanagi Y, Nakata M, Ishid O, Iwatsuru M, Tsuchiya S (1996) Direct measurement of th extravasation of polyethylene glycol-coated liposomes into soli tumour tissue by *in vivo* fluorescence microscopy. *Int J Pharmac* **144:** 11–17

Wasserheit C, Frazein A, Oratz R, Sorich J, Downey A, Hochster H Chachoua A, Wernz J, Zeleniuch-Jacquotte A, Blum R, Speyer J (199 Phase II trial of paclitaxel and cisplatin in women with advanced brea cancer: an active regimen with limiting neurotoxicity. *J Clin Oncol* 1 1993–1999

Weiss RB, Donehower RC, Wiernik PH, Ohnuma T, Gralla RJ, Trump DI Baker Jr JR, Van Echo DA, Von Hoff DD, Leyland-Jones (1990) Hypersensitivity reactions from taxol. *J Clin Oncol* 1263–1268

Yokoyama M, Miyauchi M, Yamada N, Okano T, Sakurai Y, Kataoka K Inoue S (1990) Polymer micelles as novel drug carrier:adriamycin conjugated poly(ethylene glycol)-poly(aspartic acid) block copolyme *J Control Rel* **11:** 269–278

Yokoyama M, Okano T, Sakurai Y, Ekimoto H, Shibazaki C, Kataoka K (1991) Toxicity and antitumour activity against solid tumours of micelle forming polymeric anticancer drug and its extremely long circulation i blood. *Cancer Res* **51:** 3229–3236

Yokoyama M, Okano T, Sakurai Y, Fukushima S, Okamoto K, Kataoka K (1999) Selective delivery of adriamycin to a solid tumour using polymeric micelle carrier system. *J Drug Target* **7:** 171–186

British Journal of Cancer (2005) 93, 678–687

www.bjcancer.com

Cisplatin-incorporating polymeric micelles (NC-6004) can reduce nephrotoxicity and neurotoxicity of cisplatin in rats

H Uchino[1], Y Matsumura*[,1], T Negishi[1], F Koizumi[1], T Hayashi[2], T Honda[3], N Nishiyama[4], K Kataoka[4], S Naito[5] and T Kakizoe[6]

[1]Investigative Treatment Division, National Cancer Center Research Institute East, 6-5-1 Kashiwanoha, Kashiwa, Chiba 277-8577, Japan; [2]NanoCarrier Co., Ltd, 5-4-19 Kashiwanoha, Kashiwa, Chiba 277-0882, Japan; [3]Department of Anatomy and Histology, Fukushima Medical University School of Medicine, 1-Hikariga-oka, Fukushima, Fukushima 960-1247, Japan; [4]Department of Materials Science and Engineering, Graduate School of Engineering, The University of Tokyo, 7-3-1 Hongo, Bunkyo-ku, Tokyo 113-8656, Japan; [5]Department of Urology, Graduate School of Medical Sciences, Kyushu University, 3-1-1 Maidashi, Higashi-ku, Fukuoka, Fukuoka 812-8582, Japan; [6]National Cancer Center, 5-1-1 Tsukiji, Chuo-ku, Tokyo 104-0045, Japan

In spite of the clinical usefulness of cisplatin (CDDP), there are many occasions in which it is difficult to continue the administration of CDDP due to its nephrotoxicity and neurotoxicity. We examined the incorporation of CDDP into polymeric micelles to see if this allowed the resolution of these disadvantages. Cisplatin was incorporated into polymeric micelles through the polymer–metal complex formation between polyethylene glycol poly(glutamic acid) block copolymers and CDDP (NC-6004). The pharmacokinetics, pharmacodynamics, and toxicity studies of CDDP and NC-6004 were conducted in rats or mice. The particle size of NC-6004 was approximately 30 nm, with a narrow size distribution. In rats, the area under the curve and total body clearance values for NC-6004 were 65-fold and one-nineteenth the values for CDDP ($P<0.001$ and 0.01, respectively). In MKN-45-implanted mice, NC-6004 tended to show antitumour activity, which was comparable to or greater than that of CDDP. Histopathological and biochemical studies revealed that NC-6004 significantly inhibited the nephrotoxicity of CDDP. On the other hand, blood biochemistry revealed transient hepatotoxicity on day 7 after the administration of NC-6004. Furthermore, rats given CDDP showed a significant delay ($P<0.05$) in sensory nerve conduction velocity in their hind paws as compared with rats given NC-6004. Electron microscopy in rats given CDDP indicated the degeneration of the sciatic nerve, but these findings were not seen in rats given NC-6004. These results were presumably attributable to the significantly reduced accumulation of platinum in nerve tissue when NC-6004 was administered ($P<0.05$). NC-6004 preserved the antitumour activity of CDDP and reduced its nephrotoxicity and neurotoxicity, which would therefore seem to suggest that NC-6004 could allow the long-term administration of CDDP where caution against hepatic dysfunction must be exercised.

British Journal of Cancer (2005) **93,** 678–687. doi:10.1038/sj.bjc.6602772 www.bjcancer.com
Published online 13 September 2005

Keywords: cisplatin; polymeric micelle; EPR effect; neurotoxicity

Cisplatin (*cis*-dichlorodiammineplatinum (II): CDDP) is a key drug in the chemotherapy for cancers, including lung, gastrointestinal, and genitourinary cancer (Roth, 1996; Boulikas and Vougiouka, 2004). However, we often find that it is necessary to discontinue treatment with CDDP due to its adverse reactions, for example, nephrotoxicity and neurotoxicity, despite its persisting effects (Pinzani *et al*, 1994). Platinum (Pt) analogues, for example, carboplatin and oxaliplatin (Cleare *et al*, 1978), have been developed to date to overcome these CDDP-related disadvantages. Consequently, these analogues are becoming the standard drugs for ovarian cancer (du Bois *et al*, 2003) and colon cancer (Cassidy *et al*, 2004). However, those regimens including CDDP are considered to constitute the standard treatment for lung cancer, stomach cancer, testicular cancer (Horwich *et al*, 1997), and urothelial cancer (Bellmunt *et al*, 1997). Therefore, the development of a drug delivery system (DDS) technology is anticipated, which would offer the better selective accumulation of CDDP into solid tumours while lessening its distribution into normal tissue.

Drug delivery system targeting involves two concepts: active targeting and passive targeting. Active targeting aims drug targeting through antigen–antibody reactions and specific bindings between molecules, for example, receptor and ligand. On the other hand, passive targeting is an approach in which the drug accumulates in tumour tissue using the pathophysiological characteristics of solid tumours such as the hyperplasia of tumour vasculature which generally occurs in solid tumours, but which is not seen in a comparable way in lymph nodes. Marked vascular hyperpermeability is also found in the tumour vasculature, and the combination of hyperplasia and hyperpermeability facilitate the extravasation of high-molecular-weight polymers or nanoparticles, which are less prone to leak from intact vasculature, and which can be retained in solid tumour tissue for a longer time (enhanced permeability and retention effect (EPR) effect) (Matsumura and Maeda, 1986; Maeda and Matsumura, 1989; Maeda, 2000, 2001). This effect allows passive targeting of macromolecules with a high blood retention profile into the site of tumour.

Simple polymerisation only is not sufficient to bring about the EPR effect, and strategies are also required to suppress trapping by

*Correspondence: Dr Y Matsumura; E-mail: yhmatsum@east.ncc.go.jp
Received 13 July 2005; revised 5 August 2005; accepted 9 August 2005; published online 13 September 2005

the reticuloendothelial system (RES) and to enhance the blood retention profile (Klibanov *et al*, 1990, 1991; Allen, 1994; Gabizon *etal*, 1996; Lasic, 1996). Polyethylene glycol-tagged liposomal adriamycin (Doxil®) has recently been reported as a clinical success (Orditura *etal*, 2004). We have recently been conducting research dedicated to the development of polymeric micelles capable of incorporating anticancer drugs (Yokoyama *et al*, 1990, 1991, 1999). The Phase I clinical trial of adriamycin-incorporating polymeric micelles has been completed (Matsumura *et al*, 2004). Furthermore, in an animal model, the plasma and tumour area under the curve (AUC) values for taxol-incorporating polymeric micelle (NK105) showed 85- and 25-fold increases, respectively, as compared with those for taxol. Therefore, NK105 showed significant enhancement ($P<0.001$) of the antitumour activity of free taxol and a significant reduction ($P<0.05$) in its neurotoxicity (Hamaguchi *et al*, 2005). Based on these results, the Phase I clinical trial of NK105 is currently being conducted at the National Cancer Center Hospital, Tokyo. We have also been conducting research dedicated to the development of CDDP-incorporating polymeric micelles and have made a number of improvements, in the *in vivo* antitumour activity, reduction of nephrotoxicity, particle size, and particle size distribution as variables (Nishiyama and Kataoka, 2001; Nishiyama *et al*, 2001). Consequently, we discovered that block copolymers, which react with CDDP, acquire a long blood retention profile with the use of polyethylene glycol poly(glutamic acid) block copolymers (PEG-P(Glu)) (Nishiyama *et al*, 2003). In the present study, we used the final development of the technology to prepare CDDP-incorporating polymeric micelles (NC-6004) in an attempt to investigate the following objectives: (1) calculation of pharmacokinetic (PK) parameters in a detailed PK study of CDDP and NC-6004 in rats; (2) a comparison between CDDP and NC-6004 with respect to their antitumour activity in a human cancer cell line; and (3) a detailed comparison between CDDP and NC-6004 with respect to nephrotoxicity and neurotoxicity, which constitute the dose-limiting factors of CDDP.

MATERIALS AND METHODS

Materials

Cisplatin was purchased from WC Heraeus GmbH & Co., KG (Hanau, Germany). γ-Benzyl-L-glutamate *N*-carboxy anhydride was purchased from a supplier. *N,N*-dimethylformamide and 3-(4,5-dimethylthiazol-2-yl)-2,5-diphenyltetrazolium bromide were purchased from Wako Pure Chemical Co., Inc. (Osaka, Japan). α-Methoxy-ω-aminopropyl polyethylene glycol ($CH_3O-PEG-CH_2CH_2CH_2-NH_2$; MW = 12 000) was purchased from NOF Corporation (Tokyo, Japan).

Following cell lines, MKN-45, MKN-28, EJ-1, J82, MBT-2, colo201, colo320, HT-29, A549, EBC-1, PC-14, and MCF-7 cells were purchased from the American Type Culture Collection.

Female BALB/*c nu/nu* mice were purchased from SLC (Shizuoka, Japan). Female Sprague-Dawley rats were purchased from Charles River Japan (Kanagawa, Japan). All animal procedures were performed in compliance with the guidelines for the care and use of experimental animals, which had been drawn up by the Committee for Animal Experimentation at the National Cancer Center; these guidelines meet the ethical standards required by law and also comply with the guidelines for the use of experimental animals in Japan and the UKCCCR guidelines (UKCCCR, 1998).

Preparation of PEG-P(Glu) and preparation of CDDP-incorporating polymeric micelles (NC-6004)

Polyethylene glycol-P(Glu) block copolymers were synthesised according to the slightly modified procedure of the previously reported synthetic method of PEG-P(Asp) (Nishiyama and Kataoka, 2001). γ-Benzyl L-glutamate *N*-carboxy anhydride was polymerised in *N,N*-dimethylformamide, initiated with the NH_2 amino group of $CH_3O-PEG-CH_2CH_2CH_2NH_2$, to obtain PEG-poly(γ-benzyl L-glutamate) block copolymers (PEG-PBLG). The polymerisation degree of PBLG was determined to be 40 by comparing proton ratios between PEG ($-OCH_2CH_2-$: $\delta = 3.7$ p.p.m.) and phenyl groups of PBLG ($-CH_2C_6H_5$: $\delta = 7.3$ p.p.m.) in ^{1}H NMR measurement (Mercury plus 300 (Varian Technologies); solvent: DMSO-d_6; and temperature: 25°C). The benzyl group was deprotected by mixing with 0.5 N NaOH at ambient temperature to obtain PEG-P(Glu) as a sodium salt.

Cisplatin-incorporating polymeric micelles (NC-6004) were prepared according to the slightly modified procedure of the previously reported synthetic method of CDDP-incorporating polymeric micelles (Nishiyama *et al*, 2003). Briefly, the sodium salt of PEG-P(Glu) and CDDP were dissolved in distilled water ([Glu] = 4.7 mmol l^{-1}; [CDDP]/[Glu] = 1.0) and were allowed to react for 72 h. NC-6004 thus prepared was purified with ultrafiltration (molecular weight cutoff size: 100 000). The size distribution of NC-6004 was evaluated by dynamic light scattering (DLS) at 23°C using the NICOMP 380 ZLS particle sizer (Particle Sizing Systems, Santa Barbara, CA).

Release of CDDP from NC-6004 dissolved in saline

NC-6004 was dissolved in saline and was then incubated at 37°C. In all, 80 μl of the solution was then harvested at 3, 6, 24, and 96 h after the onset of incubation. The release of CDDP from NC-6004 in the solution harvested at 37°C was quantified by gel permeation chromatography (column: Waters Ultrahydrogel 500 (ϕ7.8 × 300 mm); Waters GPC system equipped with a UV detector (310 nm); and eluent: 10 mmol l^{-1} phosphate-buffered 50 mmol l^{-1} NaCl solution).

In vitro cytoxicity

Various human cancer cell lines were evaluated in the present study. The cell lines were maintained in monolayer cultures in Dulbecco's modified Eagle's medium containing 10% (v v^{-1}) focal calf serum and 600 mg l^{-1} glutamine. WST-8 Cell Counting kit-8 (Dojindo, Kumamoto, Japan) was used for cell proliferation assay. In all, 2000 cells of each cell line in 90 μl of culture medium were plated in 96-well plates and were then incubated for 24 h at 37°C. Serial dilutions of CDDP and NC-6004 in a volume of 10 μl were added, and the cells incubated for 48 or 72 h. All dates were expressed as mean ± s.e. of triplicate of the date triplicate cultures. The data were then plotted as a percentage of the data from the control cultures, which were treated identically to the experimental cultures, except that no drug was added.

Pharmacokinetics and pharmacodynamics of CDDP and NC-6004

Under isoflurane anaesthesia, a polyethylene catheter was inserted into the right internal jugular vein of female Sprague-Dawley female rats. Rats ($n = 3$) were given a single intravenous (i.v.) injection of CDDP (5 mg kg^{-1}) or NC-6004 (an equivalent dose of 5 mg kg^{-1} CDDP) via the tail vein. At 5, 15, and 30 min, as well as at 1, 4, 12, 24, and 48 h after injection of each drug, blood (0.2 ml) was collected into a heparinised microtube via the polyethylene catheter. The blood samples were centrifuged (1000 g) for 10 min at room temperature to obtain the plasma. The plasma samples were stored below −80°C until the analysis. In a tissue distribution study, rats were injected i.v. with CDDP (5 mg kg^{-1}) or NC-6004 (an equivalent dose of 5 mg kg^{-1} CDDP) via the tail vein, and were then killed in groups of three animals at 10 min, at 1, 6, 24, and 48 h, and on day 7 day after injection of each drug under intraperitoneal pentobarbital anaesthesia (50 mg kg^{-1}). Various organs (kidney, liver, spleen, heart, lung, small intestine, colon,

and stomach) were dissected. The organ samples were stored below −80°C until the analysis. Female BALB/*c* mice were inoculated subcutaneously on the back with 10^6 MKN-45 cells (UKCCCR, 1998). After 10 days, when the tumour size had reached approximately 50 mm^2, mice were injected i.v. with CDDP (5 mg kg^{-1}) or NC-6004 (an equivalent dose of 5 mg kg^{-1} CDDP) via the tail vein and were then killed in groups of three animals at 10 min, at 1, 6, 24, and 48 h, and on day 7 after injection of each drug. The tumours were dissected and stored below −80°C until the analysis. The plasma samples were diluted with 0.1 N HCl, vortexed, and analysed for elemental Pt by frameless atomic absorption spectrophotometry (FAAS). The tissue samples were decomposed by heating in concentrated nitric acid, evaporated to dryness, and redissolved in 0.1 N HCl. Elemental Pt was measured by FAAS.

The PK parameters were calculated using noncompartmental analysis (WinNonlin standard software, version 3.1; Pharsight Corporation, Palo Alto, CA, USA). The following PK parameters were obtained: AUC, maximum Pt concentration (C_{max}), time to obtain C_{max} (T_{max}), total body clearance (CL_{tot}), terminal half-life of Pt ($t_{1/2}z$), and steady-state volume of distribution (V_{ss}). The area under the tumour concentration–time curve (tumour AUC) was calculated based on the trapezoidal rule up to 48 h. The parameters were calculated using the following equations:

$$AUC_{0-t}$$

was calculated by the trapezoidal rule to the last measurable data point:

$$AUC_{0-inf.} = \int_0^\infty C(t)dt$$

$$t_{1/2}z(\text{terminal half-life}) = 0.693/\lambda z$$

λz: first-order rate constant associated with terminal portion of the curve)

$$CL_{tot} = \text{Dose}/AUC_{0-inf.}$$

$$V_{ss} = MRT \times CL_{tot}(MRT : \text{mean residence time})$$

In vivo antitumour activity

Antitumour activity was evaluated using nude mice implanted with a human gastric cancer cell line MKN-4. BALB/*c nu/nu* female mice (aged 6 weeks) were inoculated subcutaneously with 10^6 MKN-45 cells on the right dorsal skin. After 3 days, when tumour diameter had reached approximately 3 mm, tumour-bearing mice were allocated randomly to drug administration groups of six animals each. The drugs were administered as follows: animals in the CDDP group were given doses of 0.5, 2.5, 5 mg kg^{-1}; animals in the NC-6004 group were given doses of 0.5, 2.5, and 5 mg kg^{-1}; and animals in the control group were given the 5% glucose solution. Cisplatin or NC-6004 was administered to mice at any of the above dose levels per dose every 3 days. Antitumour activity was evaluated in terms of tumour size by measuring two orthogonal diameters ($a \times b$: a, long diameter; b, short diameter) at various time points. Animals were killed by cervical dislocation when the tumour size reached approximately 15 mm (UKCCCR, 1998). Changes in body weight were also monitored for the mice which were used in the present study.

Nephrotoxicity and hepatotoxicity of CDDP and NC-6004

Under isoflurane anaesthesia, five groups of Sprague–Dawley female rats (aged 6 weeks; 185–215 g initial body weight) were given a single i.v. injection of 5% glucose ($n = 8$), CDDP at a dose of 10 mg kg^{-1} ($n = 12$), NC-6004 at a dose of 10 mg kg^{-1} on a CDDP basis ($n = 13$), or NC-6004 at a dose of 15 mg kg^{-1} on a CDDP basis ($n = 8$). Samples of blood and major organs were taken on day 7 after administration (UKCCCR, 1998). In the case of administering NC-6004 at a dose of 10 mg kg^{-1} on a CDDP basis, five samples of blood and major organs were taken on day 14 after administration. The organs were immersed in 10% formalin solution. In each blood sample, plasma concentrations of blood urea nitrogen (BUN), creatinine, glutamic oxaloacetic transaminase (GOT), and glutamic pyruvic transaminase (GPT) were measured by SRL Laboratories (Tokyo, Japan). In addition, WBC and platelet were counted for blood samples 7 and 14 days after each drug administration in SRL Laboratories (Tokyo, Japan).

Evaluation of neurotoxicity

The severity of neurotoxicity was assessed by electrophysiological and histopathological procedures. Under isoflurane anaesthesia, rats ($n = 5$) were given CDDP (2 mg kg^{-1}), NC-6004 (an equivalent dose of 2 mg kg^{-1} CDDP), or 5% glucose, all i.v., twice a week, to a total of 11 administrations. Electrophysiological measurements were conducted at week 6 after the first administration, using the method described previously (McKeage *et al*, 1994; Screnci *et al*, 2000). Under light anaesthesia with phenobarbital, responses were evoked by stimulating the sciatic nerve at its notch and the tibial nerve at the ankle of the right hind paw, using a percutaneous needle electrode. The plantar muscle H- and M-waves were recorded using a pair of superficial silver–silver chloride electrodes applied to the sole and dorsum of the hind paw. H-response-related sensory nerve conduction velocity (SNCV) was calculated by dividing the distance between the stimulation sites at the sciatic notch and ankle by the difference in H-response latency after stimulation at the ankle and sciatic notch. M-response-related motor nerve conduction velocity (MNCV) was calculated by dividing the distance between the stimulation sites at the sciatic notch and ankle by the difference in M-response latency after stimulation at the sciatic notch and ankle. At week 7 after the initial administration, rats under deep anaesthesia with phenobarbital were subjected to intracardiac catheterisation and were rinsed with saline, followed by perfusion with 4% glutaraldehyde in 0.12 M PBS. Subsequently, a segment of the sciatic nerve was carefully removed. One part of the sciatic nerve was post-fixed with 4% glutaraldehyde in 0.12 M PBS for 24 h and was then embedded in epoxy resin as described previously (Cavaletti *et al*, 1992). The remaining parts of the sciatic nerve were immersed in a 10% formalin solution. Semi-thin (1 μm thick) and thin sections were prepared from the resin-embedded sciatic nerve for light microscopic observation and electron microscopic observation, respectively.

To determine the Pt concentration in the sciatic nerve, rats were given CDDP (5 mg kg^{-1}, $n = 5$), NC-6004 (an equivalent dose of 5 mg kg^{-1} CDDP, $n = 5$), or 5% glucose ($n = 2$), all i.v. twice a week, to a total of four administrations. On day 3 after the final administration, a segment of the sciatic nerve was removed. The removed sciatic nerve was prepared for ICP-MS analysis as described previously (Screnci *et al*, 2000). Briefly, the nerve was immersed in 1 ml of 70% nitric acid overnight. On the next day, the nerve was digested for 2 h at 90°C and Milli-Q was then added to a final volume of 5 ml. Finally, the Pt concentration in the sample solution was analysed with an ICP-MS spectrometer (SPQ 9000; Seiko Instruments Inc., Tokyo, Japan).

Statistical analysis

Data on therapeutic efficacy and body weight change were expressed as the mean ± s.e. The other data were expressed as the mean ± s.d. The statistical significance of differences in therapeutic efficacy and body weight change between two administration groups was calculated by repeated-measured

analysis of variance (ANOVA). The statistical significance of differences in other data between two administration groups was calculated with the Student's *t*-test. All data were calculated with StatView® Software, version 5 (ABACUS Concepts, Berkeley, CA). A value of $P<0.05$ was considered statistically significant.

RESULTS

Preparation and characterisation of CDDP-incorporating polymeric micelles (NC-6004)

Cisplatin-incorporating polymeric micelles (NC-6004) consist of CDDP and PEG–P(Glu) (Figure 1A). Furthermore, NC-6004 consists of PEG, a hydrophilic chain which constitutes the outer shell of the micelles, and the coordinate complex of P(Glu) and CDDP, a polymer–metal complex-forming chain which constitutes the inner core of the micelles. The molecular weight of PEG–P(Glu) as a sodium salt was approximately 18 000 (PEG: 12 000; P(Glu): 6000). The CDDP-incorporated polymeric micelles were clearly discriminated from typical micelles from amphiphilic block copolymers. The driving force of the formation of the CDDP-incorporated micelles is the ligand substitution of Pt(II) atom from chloride to carboxylate in the side chain of P(Glu). The molar ratio of CDDP to the carboxyl groups in the copolymers was 0.71 (Nishiyama *et al*, 2003). A narrowly distributed size of polymeric micelles (30 nm) was confirmed by the DLS measurement

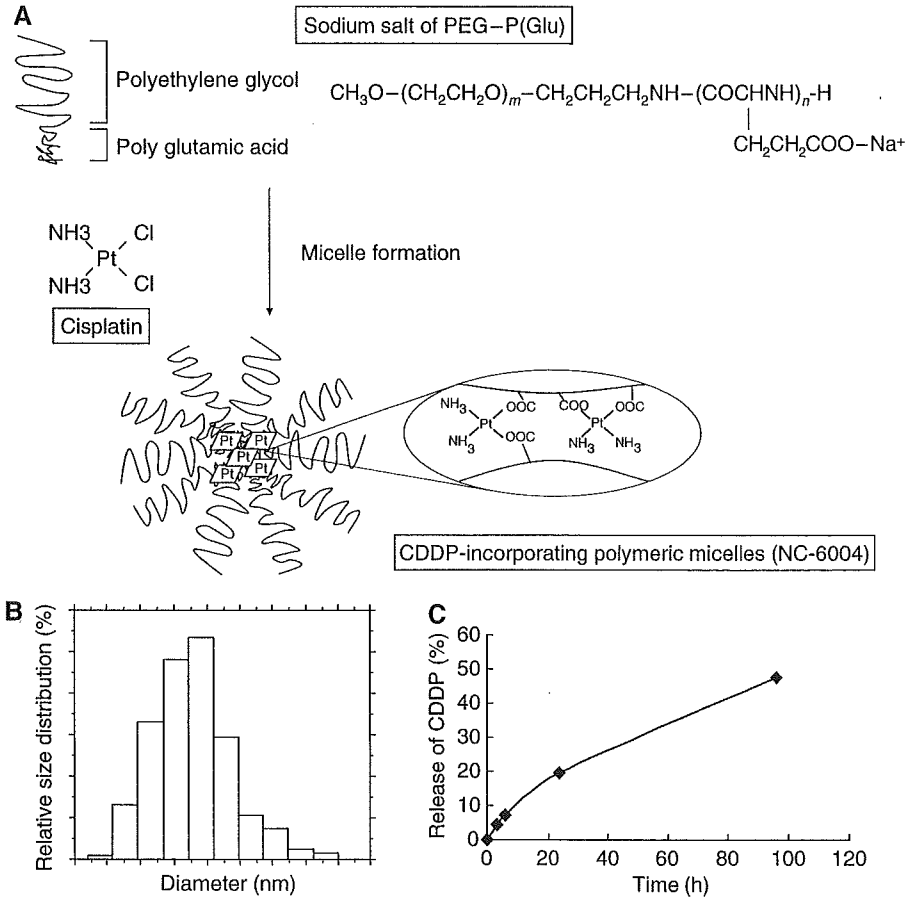

Figure 1 Preparation and characterisation of CDDP-incorporating polymeric micelles (NC-6004). (**A**) Chemical structures of CDDP and PEG–P(Glu) block copolymers, and the micellar structures of CDDP-incorporating polymeric micelles (NC-6004). (**B**) The particle size distribution of NC-6004 measured by the dynamic light-scattering method. The mean particle size of NC-6004 was approximately 30 nm. (**C**) Release of CDDP from NC-6004 in saline at 37°C.

Table 1 Pharmacokinetic parameter estimates for CDDP and NC-6004 in rats (see text for definitions of parameters)

Compound	Rat	T_{max}[a] (h)	C_{max}[a] ($\mu g\,ml^{-1}$)	$t_{1/2}z$ (h)	AUC_{0-t} ($\mu g\,h\,ml^{-1}$)	$AUC_{0-inf.}$ ($\mu g\,h\,ml^{-1}$)	CL_{tot} ($ml\,h^{-1}\,kg^{-1}$)	$MRT_{0-inf.}$ (h)	V_{ss} ($l\,kg^{-1}$)
CDDP	Mean s.d.	0.083	11.67 0.57	34.50 16.14	20.47 2.25	75.73 26.13	70.67 20.34	46.57 22.38	3.00 0.61
NC-6004	Mean s.d.	0.50	89.90 4.29	6.43 0.55	1325.90 77.85	1335.47 75.99	3.77 0.21	10.67 0.15	0.04 0.0023

The pharmacokinetic parameters were calculated after fitting to a noncompartment model using WinNonlin program. [a]For CDDP group, T_{max} represents time of maximum concentration.

(Figure 1B). Also, the static light scattering (SLS) measurement revealed that the CDDP-loaded micelles showed no dissociation upon dilution and the CMC was less than 5×10^{-7}, suggesting remarkable stability compared with typical micelles from amphiphilic block copolymers (Nishiyama *et al.* 1999). It is assumed that the interpolymer crosslinking by Pt(II) atom might contribute to stabilisation of the micellar structure.

The release rates of CDDP from NC-6004 were 19.6 and 47.8% at 24 and 96 h, respectively (Figure 1C). Therefore, the release of CDDP was as slow as the previously reported release (Nishiyama *et al*, 2003). In distilled water, furthermore, NC-6004 was stable without releasing CDDP (data not shown).

Pharmacokinetics and pharmacodynamics

Frameless atomic absorption spectrophotometry could measure serum concentrations of Pt up to 48 h after i.v. injection of NC-6004, but could measure them only up to 4 h after i.v. injection of CDDP. NC-6004 showed a very long blood retention profile as compared with CDDP. The AUC_{0-t} and C_{max} values were significantly higher in animals given NC-6004 than in animals given CDDP, namely, 65- and 8-fold, respectively ($P<0.001$ and 0.001, respectively) (Table 1, Figure 2A). Furthermore, the CL_{tot} and V_{ss} values were significantly lower in animals given NC-6004 than in animals given CDDP, that is, one-nineteenth and one-seventy-fifth, respectively ($P<0.01$ and 0.01, respectively) (Table 1).

Regarding the concentration–time profile of Pt in various tissues after i.v. injection of CDDP or NC-6004, all organs measured exhibited the highest concentrations of Pt within 1 h after administration in all animals given CDDP (Figure 2B). Furthermore, animals given NC-6004 exhibited the highest tissue concentrations of Pt in the liver and spleen at late time points (24 and 48 h after administration, respectively). However, the concentrations decreased on day 7 after administration (Figure 2C). In addition, and in a similar manner to other drugs which are incorporated in polymeric carriers, NC-6004 demonstrated accumulation in organs of the reticuloendothelial system, for example, liver and spleen. At 48 h after administration, tissue concentrations of Pt in the liver and spleen were 4.6- and 24.4-fold higher for NC-6004 than for CDDP. On the other hand, a marked increase in tissue Pt concentration was observed immediately after administration in the kidneys of animals given CDDP. Renal Pt concentration at 10 min and 1 h after administration were 11.6- and 3.1-fold lower, respectively, in animals given NC-6004 than in animals given CDDP. Furthermore, the maximum concentration (C_{max}) in the kidney was 3.8-fold lower at the time of NC-6004 administration than at the time of CDDP administration.

Regarding the tumour accumulation of Pt, tumour concentrations of Pt peaked at 10 min after administration of CDDP. On the other hand, tumour concentrations of Pt peaked at 48 h after administration of NC-6004 (Figure 2D). The maximum concentration (C_{max}) in tumour was 2.5-fold higher for NC-6004 than for CDDP ($P<0.001$). Furthermore, the tumour AUC was 3.6-fold higher for NC-6004 than for CDDP (81.2 and 22.6 $\mu g\,ml\,h^{-1}$ in animals given NC-6004 and CDDP, respectively).

In vitro cytotoxicity

NC-6004 was tasted on 12 human tumour cell lines derived from bladder, colon, lung, gastric, and breast cancers. The IC_{50} values of NC-6004 were 6-to 15-fold higher than those of CDDP (Table 2).

In vivo antitumour activity

BALB/*c* nude mice implanted with a human gastric cancer cell line MKN-45 showed decreased tumour growth rates after i.v. injection of CDDP and NC-6004 (Figure 3A). In the administration of CDDP,

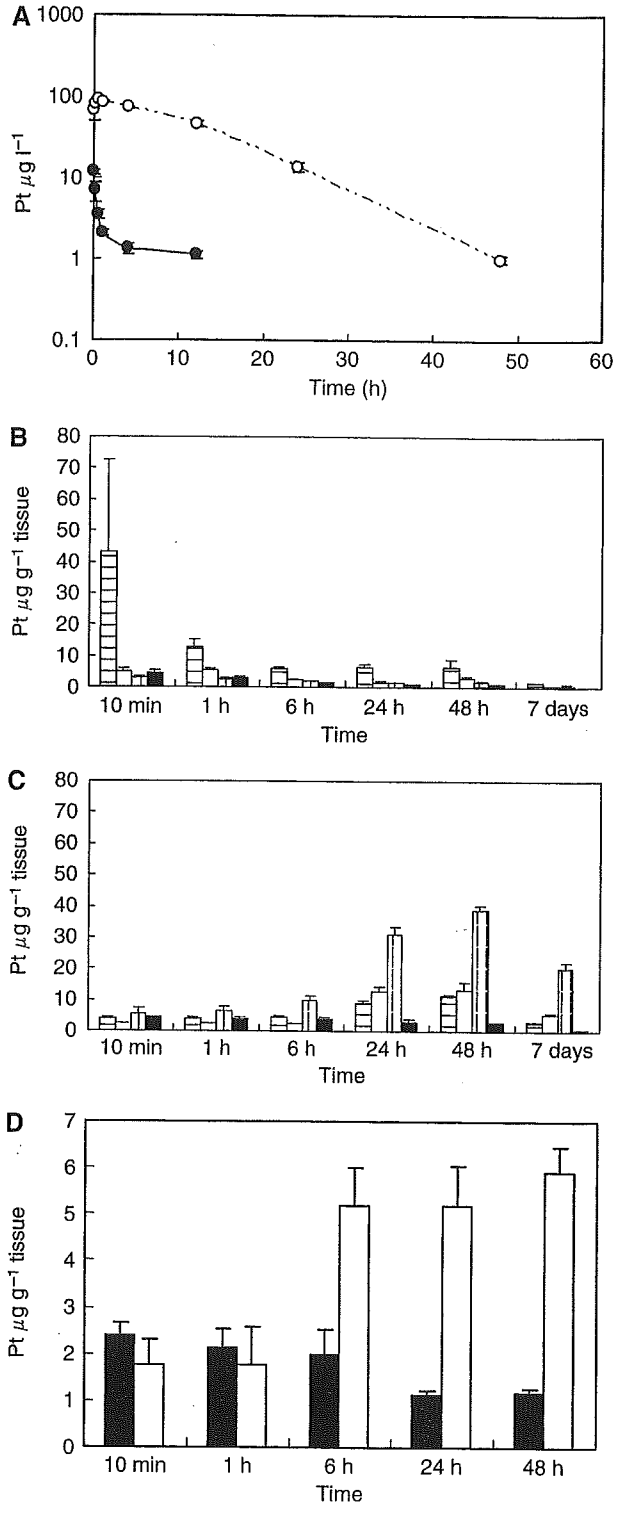

Figure 2 Time profiles of Pt concentration in the plasma and tissue distribution of Pt after a single i.v. injection of CDDP (5 mg kg^{-1}) or NC-6004 (an equivalent dose of 5 mg kg^{-1} CDDP). (**A**) Concentration–time profile of Pt in the plasma after a single i.v. injection of CDDP (●) and NC-6004 (○) in rats ($n=3$). Tissue distribution of Pt after a single i.v. injection of CDDP (**B**) and NC-6004 (**C**) in rats ($n=3$) (kidney (▤), liver (□), spleen (▥), and lung (■)). (**D**) Time profiles of Pt concentration in the MKN-45 solid tumour after a single i.v. injection of CDDP (■) and NC-6004 (□) in MKN-45 bearing BALB/*c* nude mice ($n=3$). Values are expressed as the mean ± s.d.

Table 2 IC_{50} values(μM) of CDDP and NC-6004 in various cancer cell lines

		Exposure time (h)			
		48		72	
Cancer	Cell line	CDDP	NC-6004	CDDP	NC-6004
Bladder cancer	EJ-1	2.46	25.45	1.86	18.44
	J82	2.78	42.89	2.42	20.27
	MBT-2	15.88	>100	5.67	71.67
Colon cancer	Colo201	34.77	>100	28.52	>100
	Colo320	16.32	>100	9.71	81.15
	HT-29	14.44	>100	8.83	>100
Lung cancer	A549	21.43	>100	20	>100
	EBC-1	>100	>100	9.36	84.78
	PC-14	16.81	>100	8.73	87.11
Gastric cancer	MKN-28	>100	>100	8.23	76.81
	MKN-45	7.12	68.36	6.94	43.81
Breast cancer	MCF-7	12.78	>100	5.71	54.71

the CDDP 5 mg kg^{-1} administration group showed a significant decrease ($P<0.01$) in tumour growth rate as compared with the control group. In the administration of NC-6004, NC-6004 2.5 mg kg^{-1} administration group ($P<0.05$) and 5 mg kg^{-1} administration group ($P<0.01$) showed significant decreases in tumour growth rate as compared with the control group. However, the NC-6004 administration groups at the same dose levels as CDDP showed no significant difference in tumour growth rate. The same animal model was used to repeat the study using the drugs at different dose levels, and similar tendencies were observed (data not shown). Regarding time-course changes in body weight change rate, the CDDP 5 mg kg^{-1} administration group showed a significant decrease ($P<0.001$) in body weight as compared with the control group. On the other hand, none of the NC-6004 administration groups showed a decrease in body weight as compared with the control group (Figure 3B).

Nephrotoxicity and hepatotoxicity of CDDP and NC-6004

In the CDDP 10 mg kg^{-1} administration group, four of 12 animals died from toxicity within 7 days after drug administration. No deaths occurred in the NC-6004 10 mg kg^{-1} administration group and the NC-6004 15 mg kg^{-1} administration group. Regarding renal function, the BUN concentrations on day 7 after the administration of 5% glucose, CDDP 10 mg kg^{-1}, NC-6004 10 mg kg^{-1}, and NC-6004 15 mg kg^{-1} were 20.8 ± 3.0, 65.3 ± 44.4, 20 ± 4.5, and 24.6 ± 18.2 mg dl^{-1}, respectively. The plasma concentrations of creatinine on day 7 after the administration of 5% glucose, CDDP 10 mg kg^{-1}, NC-6004 10 mg kg^{-1}, and NC-6004 15 mg kg^{-1} were 0.27 ± 0.03, 0.68 ± 0.23, 0.28 ± 0.04, and 0.45 ± 0.11 mg dl^{-1}, respectively. The CDDP 10 mg kg^{-1} administration group showed significantly higher plasma concentrations of BUN and creatinine as compared with the control group ($P<0.05$ and 0.001, respectively), with the NC-6004 10 mg kg^{-1} administration group ($P<0.05$ and 0.001, respectively), and also with the NC-6004 15 mg kg^{-1} administration group ($P<0.05$ and 0.05, respectively) (Figure 4A and B). Light microscopy indicated tubular dilation with flattening of the lining cells of the tubular epithelium in the kidney from all animals in the CDDP 10 mg kg^{-1} administration group. On the other hand, no histopathological change was observed in the kidneys from all animals in the NC-6004 10 mg kg^{-1} administration group (Figure 4C and D). Regarding hepatic function, the plasma concentrations of GOT on day 7 after the administration of 5% glucose, CDDP 10 mg kg^{-1}, NC-6004 10 mg kg^{-1}, and NC-6004 15 mg kg^{-1} were 68 ± 6.8, 65.1 ± 5.5, 106 ± 13.1, and 97 ± 16.2 IU l^{-1}, respectively. The plasma

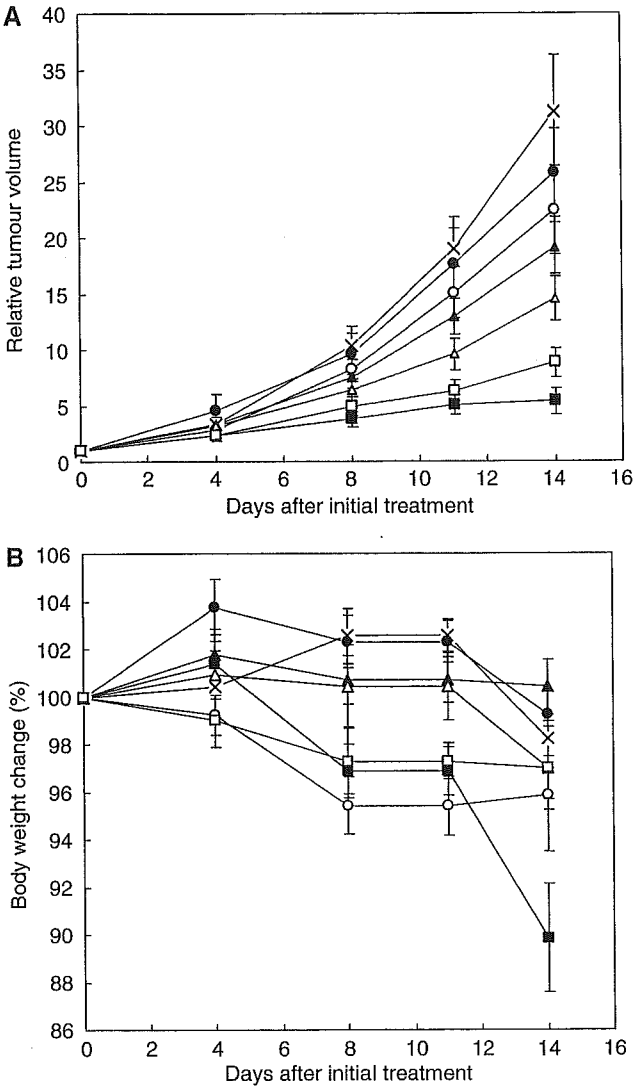

Figure 3 Relative changes in MKN-45 tumour growth rates in nude mice. (**A**) Cisplatin and NC-6004 were injected i.v. every 3 days, three administrations in total, at CDDP-equivalent doses of 0.5 mg kg^{-1} (●, ○), 2.5 mg kg^{-1} (▲, △), and 5 mg kg^{-1} (■, □), respectively. Glucose (5%) was injected in the control mice (×). (**B**) Changes in relative body weight. Data were derived from the same mice as those used in the present study. Values are expressed as the mean ± s.e.

concentrations of GPT on day 7 after the administration of 5% glucose, CDDP 10 mg kg^{-1}, NC-6004 10 mg kg^{-1}, and NC-6004 15 mg kg^{-1} were 39.6 ± 10, 32 ± 6.4, 92 ± 18.9, and 55 ± 11.3 IU l^{-1}, respectively. The CDDP 10 mg kg^{-1} administration group showed plasma concentrations of GOT and GPT which were comparable to those in the control group. However, the NC-6004 10 mg kg^{-1} administration group, which presented the same dose level as the CDDP 10 mg kg^{-1} administration group, showed significantly higher plasma concentrations of GOT and GPT ($P<0.001$ and 0.01, respectively) as compared with the control group. Furthermore, the NC-6004 15 mg kg^{-1} administration group also showed significantly higher plasma concentrations of GOT ($P<0.001$) as compared with the control group. However, the plasma concentrations of GOT and GPT on day 14 after the administration of NC-6004 10 mg kg^{-1} were comparable to those in the control group (74 ± 2.3 and 42.8 ± 5.1 IU l^{-1}, respectively) (Figure 4E). These results lead to the conjecture that rats which were given NC-6004 10 mg kg^{-1}, i.v., showed transient and reversible hepatotoxicity.

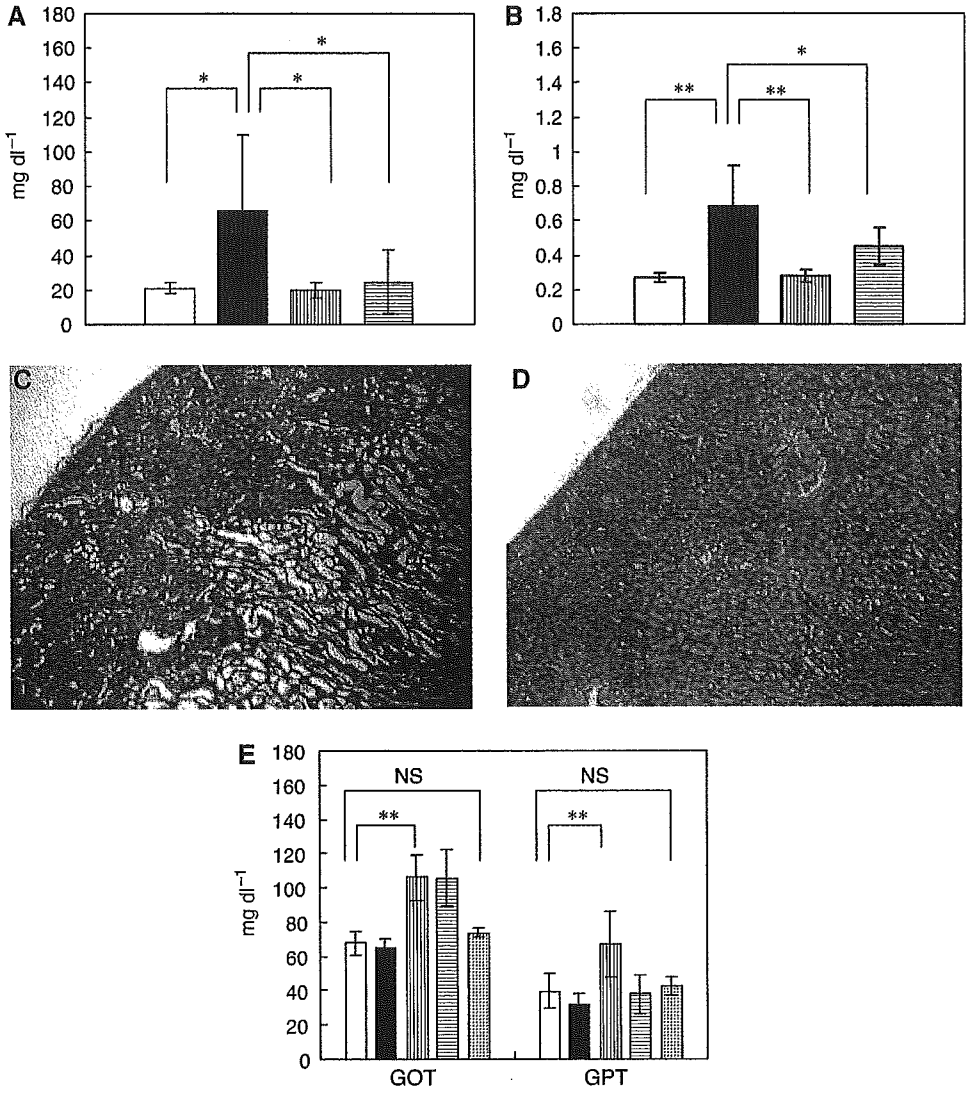

Figure 4 Nephrotoxicity and hepatotoxicity of CDDP and NC-6004. Plasma concentrations of BUN (**A**) and creatinine (**B**) were measured after a single i.v. injection of 5% glucose (□) ($n=8$), CDDP at a dose of 10 mg kg^{-1} (■) ($n=12$), NC-6004 at a dose of 10 mg kg^{-1} ($n=13$) on a CDDP basis (▥), and at a dose of 15 mg kg^{-1} on a CDDP basis (▤) ($n=8$) to rats. Histopathological changes in the kidney on day 7 after the i.v. injection of CDDP (**C**, ×4) and NC-6004 (**D**, ×4) in rats at an equivalent dose of 10 mg kg^{-1} CDDP. In rats given CDDP, widespread tubular degeneration as indicated by tubular dilation with flattening of the lining cells of tubular epithelium was seen. On the other hand, no histopathological change was observed in the kidney from all animals in the NC-6004 10 mg kg^{-1} administration group. For hepatotoxicity (**E**), the plasma concentrations of GOT and GPT were measured on day 7 after administration. When administering NC-6004 at a dose of 10 mg kg^{-1} on a CDDP basis, five of 13 blood samples were taken on day 14 after administration (▥). The other samples were taken on day 7 administration. In the group given CDDP at a dose of 10 mg kg^{-1}, four of 12 rats died within 7 days. Values are expressed as the mean ± s.d. *$P<0.05$, **$P<0.001$, NS: not significant.

Neurotoxicity of CDDP and NC-6004

Neurophysiological examination revealed that MNCVs in animals given 5% glucose, CDDP, and NC-6004 were 44.2 ± 3.5, 40.94 ± 5.08, and 40.62 ± 0.63 m s^{-1}, respectively. No significant difference was found among the groups with respect to MNCV. Furthermore, SNCVs in animals given 5% glucose, CDDP, and NC-6004 were 42.86 ± 8.07, 35.48 ± 4.91, and 43.74 ± 5.3 m s^{-1}, respectively. Animals given NC-6004 showed no delay in SNCV as compared with animals given 5% glucose. On the other hand, animals given CDDP showed a significant delay ($P<0.05$) in SNCV as compared with animals given NC-6004 (Figure 5A). In addition, histopathological examination with electron microscopy revealed degenerations, as manifested by electron photomicrographs indicating degenerative changes, for example, loss of microtubules, degeneration in the cytoplasm of Schwann cells, loss of filaments, and an irregular inner loop, in approximately 80% of myelinated segments of the sciatic nerve from animals given CDDP. On the other hand, animals given NC-6004 exhibited nearly normal electron photomicrographs of the sciatic nerve as the control animals did (Figure 5B and C). These results indicate that NC-6004 reduced peripheral neurotoxicity as compared with CDDP. Furthermore, regarding body weight change as an indication of general toxicity, furthermore, the NC-6004 administration groups showed significant inhibition of body weight decrease ($P<0.001$) as compared with the CDDP administration group ($P<0.001$) (Figure 5D).

The analysis by ICP-MS on sciatic nerve concentrations of Pt could not detect Pt in the sciatic nerve from animals given 5% glucose (data not shown). Sciatic nerve concentrations of Pt in

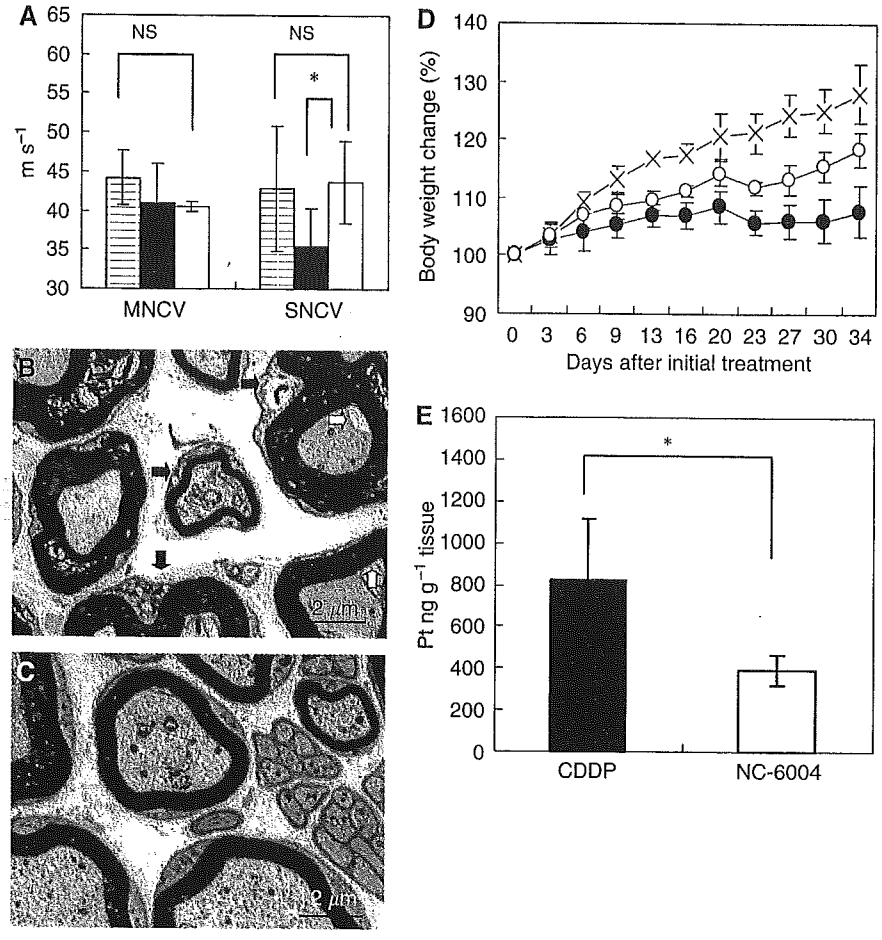

Figure 5 Neurotoxicity of CDDP and NC-6004 in rats. Rats ($n=5$) were given CDDP (2 mg kg^{-1}), NC-6004 (an equivalent dose of 2 mg kg^{-1} CDDP), or 5% glucose, all i.v. twice a week, 11 administrations in total. (**A**) Sensory nerve conduction velocity and MNCV of the sciatic nerve at week 6 after the initial administration (control (⊟), CDDP (●), and NC-6004 (□)). Histopathological changes of the sciatic nerve were examined by electron microscopy after the administration of CDDP (**B**) and NC-6004 (**C**). In rats given CDDP, widespread degenerations as indicated by loss of microtubules, loss of filaments, degeneration in the cytoplasm of Schwann cells (➡), and an irregular inner loop (⇨) were seen. On the other hand, animals given NC-6004 exhibited nearly normal electron micrographs of the sciatic nerve as the control animals. (**D**) Changes in relative body weight. Data were derived from the same rats as those used in the present study (control (×), CDDP (●), and NC-6004 (○)). (**E**) The Pt concentration in the sciatic nerve. Rats were given CDDP (■) (5 mg kg^{-1}, $n=5$), NC-6004 (□) (an equivalent dose of 5 mg kg^{-1} CDDP, $n=5$), or 5% glucose ($n=2$), all i.v. twice a week, four administrations in total. On day 3 after the final administration, a segment of the sciatic nerve was removed and the Pt concentration in the sciatic nerve was measured by ICP-MS. Body weight changes are expressed as the mean ± s.e. The other data are expressed as the mean ± s.d. *$P<0.05$, **$P<0.001$, NS: not significant.

animals given CDDP and NC-6004 were 827.2 ± 291.3 and 395.5 ± 73.1 ng g^{-1} tissue. Therefore, the concentrations were significantly ($P<0.05$) lower in animals given NC-6004 (Figure 5E). This finding is believed to be a factor which reduced neurotoxicity following NC-6004 administration as compared with the CDDP administration.

DISCUSSION

The present study indicated that CDDP-incorporating polymeric micelles (NC-6004) are stable nanoparticles with a long blood retention profile as compared with free CDDP. NC-6004 showed 6- to 15-fold less potent *in vitro* cytotoxic activity in several human cancer cell lines as compared with CDDP. These findings are considered attributable to the slow release of free CDDP in the presence of abundant chloride ions because NC-6004 contains coordination bonds between the atoms of Pt(II) of CDDP and the carboxylic group in the side chain of P(Glu). *In vivo*, however, in contrast to the *in vitro* findings, NC-6004 was found to markedly reduce nephrotoxicity and neurotoxicity – dose-limiting factors of CDDP, while preserving antitumour activity, which was equivalent to or better than that of free CDDP.

Nephrotoxicity of CDDP is considered to depend on the peak urinary CDDP concentration and on the maximum CDDP concentration in the uriniferous tubules (Levi *et al*, 1982). We consider that the reduced nephrotoxicity of NC-6004 may be explained by the following facts: (1) the tendency of micelles to be less prone to filtration by nephrons because of the NC-6004 particle size (approximately 30 nm), and (2) the much lower C_{max} value for CDDP at least in the uriniferous tubules than the value following CDDP administration. NC-6004 possibly facilitates treatment on an outpatient basis because it allows safer administration to patients with decreased renal function and requires no massive fluid replacement to protect renal tissue after the administration of CDDP.

The main neuropathy of CDDP is sensory peripheral neuropathy (van der Hoop *et al*, 1990; Gregg *et al*, 1992). A delay in SNCV due to the injury of dorsal root ganglia and peripheral nerve has previously been reported in rats given CDDP, although MNCV was

preserved in the tail and hind paws of rats (McKeage *et al*, 1994; Tredici *et al*, 1998; Meijer *et al*, 1999; Tredici *et al*, 1999). Furthermore, histopathological examination revealed degenerative changes in the sciatic nerve in similar experimental animals (Cavaletti *et al*, 1992; Tredici *et al*, 1999). In the present study, animals given NC-6004 showed no delay in the SNCV, while animals given CDDP showed a significant delay in the SNCV as compared with animals given NC-6004. Neuropathologically, neuronal degeneration, which was observed following CDDP administration, was not observed with NC-6004 administration. This result is considered attributable principally to the fact that the peripheral nerve concentration of Pt decreased to half or less following NC-6004 administration than with CDDP administration. The nervous tissue concentration of Pt at the time of NC-6004 administration decreased significantly despite the fact that the plasma AUC at the time of NC-6004 administration was high, being 65-fold higher than the plasma AUC concentration with CDDP administration. We consider that this result is attributed to the marked inhibition of Pt distribution into nervous tissue in the NC-6004 administration groups as manifested by V_{ss} of 3.00 ± 0.61 and $0.04 \pm 0.0023\,l\,kg^{-1}$ in the CDDP and NC-6004 groups, respectively. In any event, we believe that the neurotoxicity of CDDP reduced by NC-6004 allows its long-term administration.

On the other hand, transient hepatic dysfunction was observed in rats. This observation indicates the proneness of Pt to accumulate in the RES of the liver because NC-6004 is, after all, said and done, a macromolecule, although preserving a stealth effect through its outer shell of PEG. We consider that caution should be exercised against hepatic dysfunction in conducting a clinical trial of NC-6004 in the future. However, the accumulation of Pt was lower following NC-6004 administration due to a decrease in V_{ss} in other organs including nerve. As shown by changes in body weight in multiple dose studies in rats, the NC-6004 administration groups have been demonstrated to show a smaller decrease in body weight as compared with the CDDP administration groups. In single-dose studies, furthermore, one dose of CDDP $10\,mg\,kg^{-1}$ was equivalent to the 50% of the lethal dose. In fact, four of 12 animals died within 7 days after administration. However, none of the eight animals in the NC-6004 group died after the administration of NC-6004 at a CDDP equivalent dose of $15\,mg\,kg^{-1}$. In terms of haematological toxicity, there was no significant difference between the CDDP and NC-6004 groups in rats (data not shown).

In murine tumour strains, CDDP-incorporating polymeric micelles showed significantly high antitumour activity (Nishiyama *et al*, 2003). In the human gastric cancer strain used in the present study, however, no significant difference was found between the NC-6004 and CDDP administration groups. A significant difference was found in antitumour activity between the NC-6004 low-dose group ($2.5\,mg\,kg^{-1}$ administration group) and the control group, while no significant difference was found between the CDDP low-dose group ($2.5\,mg\,kg^{-1}$ administration group) and the control group. Results available to date and the results from the present study lead to the consideration that the incorporation of CDDP into polymeric micelles does not reduce its antitumour activity.

Data from the present study warrant the clinical evaluation of NC-6004. We consider that the protocol for the Phase I clinical trial of NC-6004 should employ a regimen without massive i.v. drip infusion.

ACKNOWLEDGEMENTS

This work is supported by Grants-in-Aid from the Ministry of Health, Labour and Welfare of Japan. We thank Drs T Kawaguchi and K Shimada for their expert technical assistance and Mrs K Shiina for her secretarial assistance.

REFERENCES

Allen TM (1994) Long-circulating (sterically stabilized) liposomes for targeted drug delivery. *Trends Pharmacol Sci* **15:** 215–220

Bellmunt J, Ribas A, Eres N, Albanell J, Almanza C, Bermejo B, Sole LA, Baselga J (1997) Carboplatin-based *versus* cisplatin-based chemotherapy in the treatment of surgically incurable advanced bladder carcinoma. *Cancer* **80:** 1966–1972

Boulikas T, Vougiouka M (2004) Recent clinical trials using cisplatin, carboplatin and their combination chemotherapy drugs (review). *Oncol Rep* **11:** 559–595

Cassidy J, Tabernero J, Twelves C, Brunet R, Butts C, Conroy T, Debraud F, Figer A, Grossmann J, Sawada N, Schoffski P, Sobrero A, Van Cutsem E, Diaz-Rubio E (2004) XELOX (capecitabine plus oxaliplatin): active first-line therapy for patients with metastatic colorectal cancer. *J Clin Oncol* **22:** 2084–2091

Cavaletti G, Tredici G, Marmiroli P, Petruccioli MG, Barajon I, Fabbrica D (1992) Morphometric study of the sensory neuron and peripheral nerve changes induced by chronic cisplatin (DDP) administration in rats. *Acta Neuropathol (Berl)* **84:** 364–371

Cleare MJ, Hydes PC, Malerbi BW, Watkins DM (1978) Anti-tumor platinum complexes: relationships between chemical properties and activity. *Biochimie* **60:** 835–850

du Bois A, Luck HJ, Meier W, Adams HP, Mobus V, Costa S, Bauknecht T, Richter B, Warm M, Schroder W, Olbricht S, Nitz U, Jackisch C, Emons G, Wagner U, Kuhn W, Pfisterer J (2003) A randomized clinical trial of cisplatin/paclitaxel *versus* carboplatin/paclitaxel as first-line treatment of ovarian cancer. *J Natl Cancer Inst* **95:** 1320–1329

Gabizon A, Chemla M, Tzemach D, Horowitz AT, Goren D (1996) Liposome longevity and stability in circulation: effects on the *in vivo* delivery to tumors and therapeutic efficacy of encapsulated anthracyclines. *J Drug Target* **3:** 391–398

Gregg RW, Molepo JM, Monpetit VJ, Mikael NZ, Redmond D, Gadia M, Stewart DJ (1992) Cisplatin neurotoxicity: the relationship between dosage, time, and platinum concentration in neurologic tissues, and morphologic evidence of toxicity. *J Clin Oncol* **10:** 795–803

Hamaguchi T, Matsumura Y, Suzuki M, Shimizu K, Goda R, Nakamura I, Nakatomi I, Yokoyama M, Kataoka K, Kakizoe T (2005) NK105, a paclitaxel-incorporating micellar nanoparticle formulation, can extend *in vivo* antitumour activity and reduce the neurotoxicity of paclitaxel. *Br J Cancer* **92:** 1240–1246

Horwich A, Sleijfer DT, Fossa SD, Kaye SB, Oliver RT, Cullen MH, Mead GM, de Wit R, de Mulder PH, Dearnaley DP, Cook PA, Sylvester RJ, Stenning SP (1997) Randomized trial of bleomycin, etoposide, and cisplatin compared with bleomycin, etoposide, and carboplatin in good-prognosis metastatic nonseminomatous germ cell cancer: a Multiinstitutional Medical Research Council/European Organization for Research and Treatment of Cancer Trial. *J Clin Oncol* **15:** 1844–1852

Klibanov AL, Maruyama K, Beckerleg AM, Torchilin VP, Huang L (1991) Activity of amphipathic poly(ethylene glycol) 5000 to prolong the circulation time of liposomes depends on the liposome size and is unfavorable for immunoliposome binding to target. *Biochim Biophys Acta* **1062:** 142–148

Klibanov AL, Maruyama K, Torchilin VP, Huang L (1990) Amphipathic polyethylene glycols effectively prolong the circulation time of liposomes. *FEBS Lett* **268:** 235–237

Lasic DD (1996) Doxorubicin in sterically stabilized liposomes. *Nature* **380:** 561–562

Levi FA, Hrushesky WJ, Halberg F, Langevin TR, Haus E, Kennedy BJ (1982) Lethal nephrotoxicity and hematologic toxicity of *cis*-diammine-dichloroplatinum ameliorated by optimal circadian timing and hydration. *Eur J Cancer Clin Oncol* **18:** 471–477

Maeda H (2001) The enhanced permeability and retention (EPR) effect in tumor vasculature: the key role of tumor-selective macromolecular drug targeting. *Adv Enzyme Regul* **41:** 189–207

Maeda H, Matsumura Y (1989) Tumoritropic and lymphotropic principles of macromolecular drugs. *Crit Rev Ther Drug Carrier Syst* **6:** 193–210

Maeda H, Wu J, Sawa T, Matsumura Y, Hori K (2000) Tumor vascular permeability and the EPR effect in macromolecular therapeutics: a review. *J Control Rel* **65:** 271–284

Matsumura Y, Hamaguchi T, Ura T, Muro K, Yamada Y, Shimada Y, Shirao K, Okusaka T, Ueno H, Ikeda M, Watanabe N (2004) Phase I clinical trial and pharmacokinetic evaluation of NK911, a micelle-encapsulated doxorubicin. *Br J Cancer* **91:** 1775–1781

Matsumura Y, Maeda H (1986) A new concept for macromolecular therapeutics in cancer chemotherapy: mechanism of tumoritropic accumulation of proteins and the antitumor agent smancs. *Cancer Res* **46:** 6387–6392

McKeage MJ, Boxall FE, Jones M, Harrap KR (1994) Lack of neurotoxicity of oral bisacetatoamminedichlorocyclohexylamine-platinum(IV) in comparison to cisplatin and tetraplatin in the rat. *Cancer Res* **54:** 629–631

Meijer C, de Vries EG, Marmiroli P, Tredici G, Frattola L, Cavaletti G (1999) Cisplatin-induced DNA-platination in experimental dorsal root ganglia neuronopathy. *Neurotoxicology* **20**(6): 883–887

Nishiyama N, Kataoka K (2001) Preparation and characterization of size-controlled polymeric micelle containing *cis*-dichlorodiammineplatinum(II) in the core. *J Control Rel* **74:** 83–94

Nishiyama N, Kato Y, Sugiyama Y, Kataoka K (2001) Cisplatin-loaded polymer–metal complex micelle with time-modulated decaying property as a novel drug delivery system. *Pharm Res* **18:** 1035–1041

Nishiyama N, Okazaki S, Cabral H, Miyamoto M, Kato Y, Sugiyama Y, Nishio K, Matsumura Y, Kataoka K (2003) Novel cisplatin-incorporated polymeric micelles can eradicate solid tumors in mice. *Cancer Res* **63:** 8977–8983

Nishiyama N, Yokoyama M, Aoyagi T, Okano T, Sakurai Y, Kataoka K (1999) Preparation and characterization of self-assembled polymer–metal complex micelle from *cis*-dichlorodiammineplatinum(II) and poly(ethylene glycol)-poly(α,β-aspartic acid) block copolymer in an aqueous medium. *Langmuir* **15:** 377–383

Orditura M, Quaglia F, Morgillo F, Martinelli E, Lieto E, De Rosa G, Comunale D, Diadema MR, Ciardiello F, Catalano G, De Vita F (2004) Pegylated liposomal doxorubicin: pharmacologic and clinical evidence of potent antitumor activity with reduced anthracycline-induced cardiotoxicity (review). *Oncol Rep* **12:** 549–556

Pinzani V, Bressolle F, Haug IJ, Galtier M, Blayac JP, Balmes P (1994) Cisplatin-induced renal toxicity and toxicity-modulating strategies: a review. *Cancer Chemother Pharmacol* **35:** 1–9

Roth BJ (1996) Chemotherapy for advanced bladder cancer. *Semin Oncol* **23:** 633–644

Screnci D, McKeage MJ, Galettis P, Hambley TW, Palmer BD, Baguley BC (2000) Relationships between hydrophobicity, reactivity, accumulation and peripheral nerve toxicity of a series of platinum drugs. *Br J Cancer* **82:** 966–972

Tredici G, Braga M, Nicolini G, Miloso M, Marmiroli P, Schenone A, Nobbio L, Frattola L, Cavaletti G (1999) Effect of recombinant human nerve growth factor on cisplatin neurotoxicity in rats. *Exp Neurol* **159:** 551–558

Tredici G, Tredici S, Fabbrica D, Minoia C, Cavaletti G (1998) Experimental cisplatin neuronopathy in rats and the effect of retinoic acid administration. *J Neurooncol* **36:** 31–40

van der Hoop RG, van der Burg ME, ten Bokkel Huinink WW, van Houwelingen C, Neijt JP (1990) Incidence of neuropathy in 395 patients with ovarian cancer treated with or without cisplatin. *Cancer* **66:** 1697–1702

UKCCCR, PO Box 123, Kincolin's Inn Fields, London, WC2A 3PX (1998) United Kingdom Co-ordinating Committee on Cancer Research (UKCCCR) guidelines for the welfare of animals in experimental neoplasia (second edition). *Br J Cancer* **77:** 1–10

Yokoyama M, Miyauchi M, Yamada N, Okano T, Sakurai Y, Kataoka K, Inoue S (1990) Characterization and anticancer activity of the micelle-forming polymeric anticancer drug adriamycin-conjugated poly(ethylene glycol)-poly(aspartic acid) block copolymer. *Cancer Res* **50:** 1693–1700

Yokoyama M, Okano T, Sakurai Y, Ekimoto H, Shibazaki C, Kataoka K (1991) Toxicity and antitumor activity against solid tumors of micelle-forming polymeric anticancer drug and its extremely long circulation in blood. *Cancer Res* **51:** 3229–3236

Yokoyama M, Okano T, Sakurai Y, Fukushima S, Okamoto K, Kataoka K (1999) Selective delivery of adriamycin to a solid tumor using a polymeric micelle carrier system. *J Drug Target* **7:** 171–186